GUIDELINES FOR OPTIMIZING WIRELINE FORMATION TESTING AND DOWNHOLE FLUID ANALYSIS TO ADDRESS FAULT TRANSMISSIVITY IN THE CONTEXT OF RESERVOIR COMPARTMENT CONNECTIVITY

A Thesis

by

THOMAS PFEIFFER

Submitted to the Office of Graduate Studies of
Texas A&M University
in partial fulfillment of the requirements for the degree of

MASTER OF SCIENCE

December 2010

Major Subject: Petroleum Engineering

Guidelines for Optimizing Wireline Formation Testing and Downhole Fluid Analysis to Address Fault Transmissivity in the Context of Reservoir Compartment Connectivity.

GUIDELINES FOR OPTIMIZING WIRELINE FORMATION TESTING AND DOWNHOLE FLUID ANALYSIS TO ADDRESS FAULT TRANSMISSIVITY IN THE CONTEXT OF RESERVOIR COMPARTMENT CONNECTIVITY

A Thesis

by

THOMAS PFEIFFER

Submitted to the Office of Graduate Studies of
Texas A&M University
in partial fulfillment of the requirements for the degree of

MASTER OF SCIENCE

Approved by:

Chair of Committee,	David Schechter
Committee Members,	Wayne Ahr
	Gioia Falcone
Head of Department,	Stephen Holditch

December 2010

Major Subject: Petroleum Engineering

ABSTRACT

Guidelines for Optimizing Wireline Formation Testing and Downhole Fluid Analysis to Address Fault Transmissivity in the Context of Reservoir Compartment Connectivity.

(December 2010)

Thomas Pfeiffer, B.S.; M.S., Technical University of Munich

Chair of Advisory Committee: Dr. David Schechter

Reservoir fluids are rarely found in homogeneous structures having homogeneous properties. The various elements and processes of the petroleum system result in complex fluid distributions and compositions. A sound understanding of these complexities can avoid disappointing results and costly mistakes when designing the completion and production of the reservoir. The earlier these complexities are understood in the exploration phase, the better are the chances of a successful decision making process in the design phase of the project. Assessing reservoir compartment connectivity is of paramount importance for a optimal field development. Recent technological advances in wireline formation testing and sampling provide asset teams with a new methodology to evaluate in situ fluid properties and reservoir connectivity.

After a review of the technology of downhole fluid analysis (DFA), the currently available methods of modeling equilibrated fluid gradients are presented. Fluid composition equilibrium is a stationary state where all components have reached zero mass flux. A reservoir model is designed to simulate numerically equilibration processes

over geologic timescales at isothermal conditions where diffusion and gravity are the active mechanisms. A variety of initial conditions and reservoir fluid types is considered. Non-equilibrium fluid gradients and their transient behavior as they evolve towards fluid composition equilibrium are the main interest of this study. The results are compared in case studies, that are available in published literature. The modeling methods allow modeling of vertical and lateral fluid gradients.

After a discussion of the cases, this thesis gives recommendations on 1) what fluid properties should be assessed and 2) how many data points are needed to reduce the chance of misinterpretation of non-equilibrium gradients in the presence of faults. To make best use DFA data, the property that exhibits the largest gradient needs to be investigated, as it yields the greatest potential to assess connectivity. The shape of the distribution of fluid composition within a compartment is found to be an important part in investigating reservoir connectivity. During data acquisition efforts should be made to acquire enough data points to reveal this shape. In combination with the presented techniques to identify non-equilibrium conditions, this will optimize DFA data acquisition and maximize the value of the data.

ACKNOWLEDGEMENTS

I would like to thank my committee chair, Dr. David Schechter, and my committee members, Dr. Gioia Falcone, and Dr. Wayne Ahr, for their guidance and support throughout my time at Texas A&M.

I also want to extend my gratitude to Dr. Oliver Mullins and Dr. Zulfiquar Reza. Their guidance and support have enabled me to achieve above and beyond what I could have reached without them.

Finally, I would like to thank my loving wife for her encouragement, patience and love. Her ability to give our family a home wherever we are in the world is unsurpassed.

NOMENCLATURE

AAD	absolute average deviation
α	electronic absorption coefficient
D	diffusion coefficient
D_{eff}	effective diffusion coefficient
DFA	down hole fluid analysis
EoS	equation of state
FCA	fluid comparison algorithm
h_{ω}	photon energy
GOC	gas oil contact
GOR	gas oil ratio
I_i	incident light intensity
I_t	transmitted light intensity
L	half length of horizontal model
LFA	life fluid analyzer
	average chain length of mixture
N_i	chain length of component i
OD	optical density
p	pressure
R	universal gas constant

SCN	single carbon number group
T	temperature
t	time
TVD	true vertical depth
τ	tortuosity
Φ	total porosity
Φ_{eff}	effective porosity

TABLE OF CONTENTS

CHAPTER Page

LIST OF FIGURES

FIGURE Page

LIST OF TABLES

CHAPTER I

INTRODUCTION

As organic material contained in source rocks is buried, it is gradually subjected to elevated temperature and pressure. It is converted into gas and oil that will migrate into the reservoir. Different types of organic matter, also called kerogen, have the tendency to liberate different types of hydrocarbons. The burial history of the petroleum system, the liberation, migration, trapping and storage of hydrocarbons expose the fluid to various processes that account for its complexities. Even though the fluid may have time to equilibrate, there can still be large fluid gradients. As the industry spends more resources and effort in studying the fluid in the reservoir, it becomes apparent that in some cases the fluid column has not even reached equilibrium. On frequent occasions biodegradation, multiple and active charges, seal breaches, water washing, and other processes cause the fluid to be in disequilibrium (Mullins 2008). In young reservoirs the lateral diffusion may still be in a transient state (England et al. 1995). The distribution of fluid in the reservoir reflects its history. The assumption that any period of geologic time assures fluid equilibrium or even uniform fluid columns is grossly inaccurate.

The understanding of the properties of the hydrocarbon column is vital to the optimal development plan of a field. Of equal importance is to understand the reservoir architecture, i.e. the connectivity of compartments. A compartment is a part of a reservoir that needs to be penetrated by a well to be drained. Undetected barriers to the flow of the fluids may lead to disappointing production results.

This thesis follows the style of the *SPE Journal.*

A formation pressure survey may reveal compartments, but care must be taken when the survey indicates pressure communication between different parts of the reservoir. Equilibrated pressure across a barrier over geologic time does not guarantee flow communication during the production time.

Pressure transient testing used to be the method of choice to determine the distance to a sealing barrier and the size of the compartment. In deep water operations, for example, a well test can be prohibitively expensive. In other cases it may simply not possible for its associated environmental risks.

It is well known that studying fluid property distributions in the reservoir can reveal reservoir architecture. In the past, studying the fluid meant taking a blind sample, sending it to the laboratory for analysis and waiting for the results. This approach has two significant shortcomings: The time it takes for the results to become available may exceed the deadline for crucial short term decisions, which would benefit from the information gained from the sample analysis. When the laboratory fluid analysis is available it also may be too late to acquire any additional samples to clarify questions which may arise from the analysis. Taking a large number of samples to cover all bases is not very cost effective either.

DFA measures fluid properties that enable the evaluation of compartments and their connectivity, along with fluid heterogeneities. As a wireline logging service, DFA is available as soon as the data is acquired. It allows the operator to match the data acquisition to the complex nature of the reservoir as it becomes apparent during the data acquisition. Methods and workflows are available that allow for interpretation of the data

at the time of acquisition. These methods help to ensure that all the necessary information is collected while the tool is still in the well. The technology of DFA is explained briefly in Chapter II. The reader is referred to Mullins (2008) for a thorough discussion of DFA.

Seismic data and petrophysical logs give the first insight as to where to look for compartmentalization. After a formation pressure survey, gradients and excess pressure plots can be computed. Pressure communication is a necessary but insufficient condition for flow communication (Mullins 2008). In praxis: if the pressure gradients do not reveal compartments, flow communication throughout the reservoir needs to be verified by other techniques. DFA integrates with wireline formation testing. It is available in the same logging descent as the wireline formation testing tool that is used to acquire the formation pressure survey. Multiple station measurements in one or multiple wells track the fluid property changes throughout the reservoir. As the fluid distribution becomes apparent, interpretation is needed to identify the difference between an equilibrated fluid column and a fluid column that is out of equilibrium. Fluid equilibrium is a stationary state in the absence of convection. It assumes that all components have zero mass flux (Hoier and Whitson 2001). If the body of the reservoir is discontinuous because of the presence of flow barriers, it is likely that this discontinuity shows in the fluid gradient. For the fluid column to reach equilibrium large parts of the contents of the reservoir were redistributed over time by transport processes. Flow communication is necessary for these processes to reach equilibrium. Hence an equilibrated fluid column is the first indication of connectivity.

When using the distribution of fluid properties to constrain compartments it is necessary to identify the difference between an equilibrium distribution and a non-equilibrium distribution. Interpretation techniques include fluid comparison algorithm (FCA), equations of state (EoS) methods, and, most recently, asphaltene gradient modeling. These techniques can be applied as soon as the data becomes available during the acquisition of DFA. They are used to predict the fluid properties at the next measurement depth under the assumption of an equilibrium fluid distribution. If a DFA measurement does not match the prediction, the assumption of equilibrium does not hold. When spotted in at the time of acquisition, one can acquire more data to make sure the measurement is correct and complexities are well understood. A more detailed insight into these workflows and techniques will be given in Chapter III.

When the fluid column is found to be out of equilibrium, one can not necessarily conclude the presence of flow barriers. The reasons for the fluid to be out of equilibrium are plentiful. Non-equilibrium columns pose a challenge as they generally can not be modeled with analytical equations. The core of this research work is to construct a plausible model to gain insight in the development of fluid gradients between the start of the reservoir mixing process until the present day fluid distributions is reached. In this work simple reservoir models have been constructed that allow simulations over geologic time. The intent is to gain an understanding of the zeroth order physics behind these gradients. Assumptions on the origin of the fluid complexity may be made on the basis of these models. Further investigation of the case will be focused on the correct higher order phenomena that are at the bottom of the non-equilibrium. Chapter IV will

introduce the model and testing of the behavior of the model is presented. Some refinement is focused on modeling diffusion processes reasonably well. In Chapter V the model is put to work in various case studies.

In this work simple reservoir models are used to try to mimic fluid gradients that were measured in the field. The comparison of the field measurements with the results of these simple models gives insight into the timescales of diffusive mixing. It offers plausible explanations to the gradients found in real reservoirs. The effect of transmissivity of faults on the shape of the gradients is studied. The findings in this work may help to further understand fluid complexities revealed by DFA. Additionally part of the findings will lead to recommendations for data acquisition and interpretation. It will give sound reasoning in justifying extended DFA data acquisition and fluid sampling during the open hole logging program. Based on the case studies in Chapter V, recommendations for the extent of data acquisition in the presence of faults are given in Chapter VI. A conclusion of the work is presented and an outlook on future research on this topic will round off this thesis.

CHAPTER II

DOWNHOLE FLUID ANALYSIS

Understanding the properties of fluid gradients in the reservoir is one of the main interests of this research. The possibilities for complex distributions of fluid properties and composition within the reservoir are as plentiful as the number of geologic settings. Fluid properties need to be inferred from measurements. This can be done in the laboratory by sample analysis. The turnaround time for the results of a laboratory analysis can vary anywhere from several days to month. A technology that reveals fluid property variations in the reservoir as part of wireline formation testing is DFA. The fluid properties become available as soon as the data is acquired. The work of this thesis is closely linked to DFA data. The basic theory of DFA is summarized herein.

Conclusions drawn from formation fluid samples reach into all aspects of petroleum production and field development. Uncertainties in the level of how well a sample represents the real formation fluid, has lead to costly errors in the past. A reason for the lack of understanding of fluid complexities in the reservoir has been the former inability to accurately measure them. DFA overcomes this disability and has become a major part in the quest of understanding fluid complexities and reservoir architecture (Mullins 2008).

In 1992 Mullins et al. (1992) find that the electronic absorption of a variety of petroleum fluid samples exhibit the exponential Urbach absorption tail. The Urbach phenomenology relates the electronic absorption coefficient α exponentionally to the photon energy h_ω.

$$\alpha = \alpha_0 \exp\left(\frac{h_\omega}{E_0}\right) \quad \text{(II.1)}$$

E_0 is the Urbach decay width. The absorption coefficient is an intrinsic wavelength dependent property of a material.

Smits et al. (1995) explain how this theory is put to use in a optical fluid analyzer for the application of fluid sample evaluation in wireline formation testing and sampling. Lambert's law relates the transmittance, *T*, of a volume of material to the optical path length trough it, *L*, by

$$T = \frac{I_t}{I_i} = 10^{-\alpha L} \quad \text{(II.2)}$$

where α is the absorption coefficient defined above (equation II.1), I_i is the incident light intensity and I_t is the transmitted light intensity. The transmittance of petroleum fluids can vary over a wide range. It is often convenient to look at transmittance on a logarithmic scale. Hence optical density (OD) is defined as the logarithm of the ratio of transmitted and incident light intensity:

$$OD = -log\frac{It}{Ii} \quad \text{(II.3)}$$

Ten channels of a filter spectrometer measure the transmitted light intensity at various wavelengths in the visible and near infrared spectrum. The measurement of transmitted light intensity is normalized downhole with the source intensity. The tool is calibrated prior to deployment down hole by measuring it's response in the presence of a specific oil, distilled water and air.

Figure II.1 plots the optical density of a variety of fluids as a function of wave length in the visible and near infrared spectrum. The absorption spectrum of water has two peaks in the near infrared at 1450nm and 1900nm. Oil shows several small peaks around 1700nm. Making a distinction between crude oil and water is simple. All crude oils have a similar response in the near infrared spectrum, but can be distinguished by their response in the visible spectrum.

At the time, the main intention was to identify the flowing fluid phases and to ensure sample quality prior to sample acquisition. Smith et al. (1995) introduce a model that allows deriving fluid fraction calculations in the presence of two phase flow (oil and water). The model allows a calculation of the fraction of water. The fraction of oil flow is calculated as 1-waterfraction. The authors also introduce a gas detector as a separate sensor unit that accounts for the presence of gas. The results of the initial testing of the tool are discussed and a field example is presented. For the full details the reader is referred to the original publication (Smits et al. 1995).

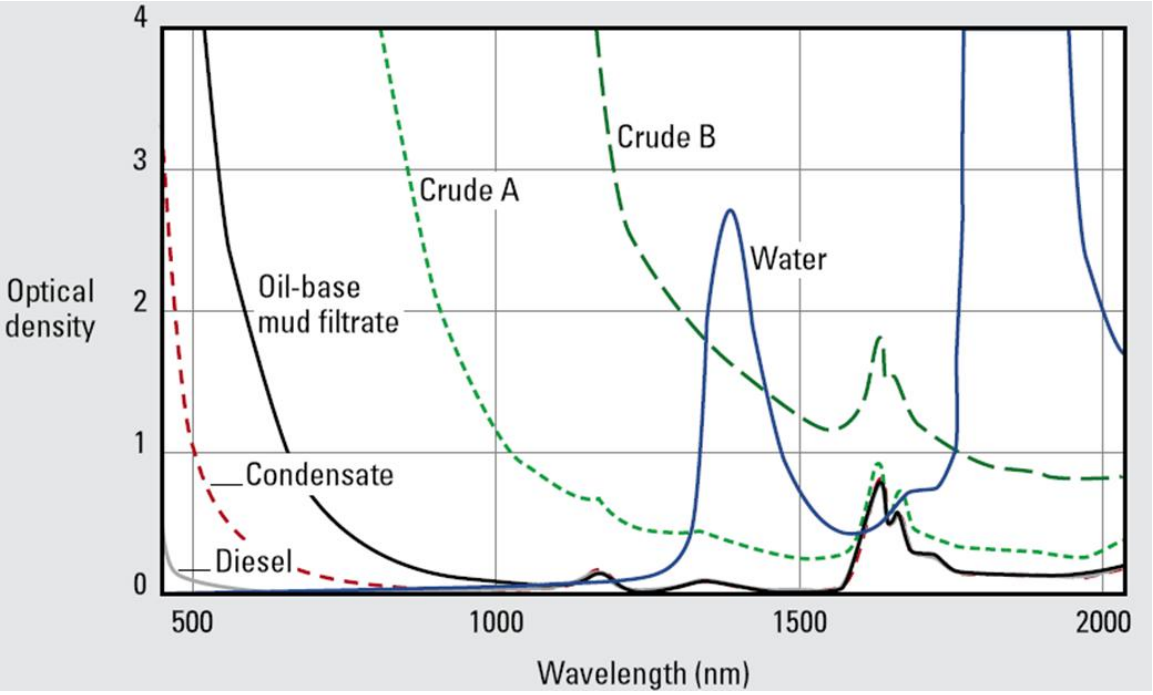

Figure II.1 – OD of various fluids against wavelength in the visible and near infrared spectrum (Smits et al. 1995).

The optical fluid analyzer as described above is able to distinguish between oil, water and gas. From its measurements it can calculate the fractions of oil, gas and water in the presence of multiphase flow using a flow model. It infers the color of the oil from its absorption in the visible spectrum. The change of color over time is an indicator of the level of drilling mud filtrate contamination. It can be modeled for single phase flow. The model allows the calculation of the miscible contamination of drilling mud filtrate when sampling oil from a formation drilled with oil based mud.

All oils exhibit an oil peak at around 1730nm in the near infrared spectrum. Methane exhibits an absorption peak at 1670nm. The peaks of a live crude oil, methane

and dead oil are shown in Figure II.2. The spectra of methane and dead oil add linearly to give the spectrum of the live oil.

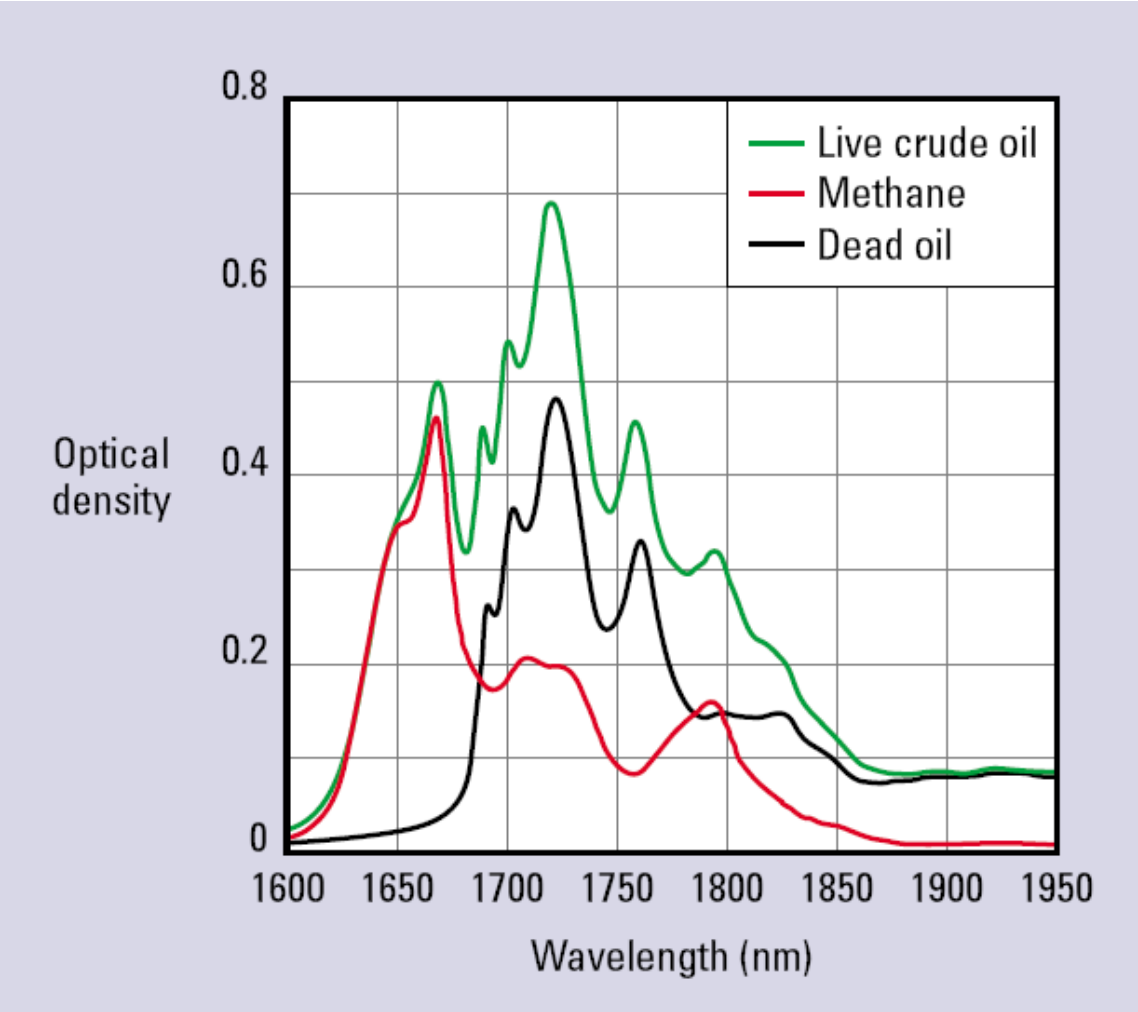

Figure II.2 – Optical density response of live oil, dead oil and methane. The methane peak helps to distinguish between oil based mud filtrate and formation oil. The spectra of methane and dead oil add linearly to give the spectrum of the live oil (Mullins et al. 2001).

The measurement of the peak height allows to infer the GOR of live oil (Mullins et al. 2001). The Live Fluid Analyzer (LFA) was the first tool that incorporated that measurement. It was intended to better approximate the mud filtrate contamination.

Mullins and Schroer (2000) present a model for the influx of reservoir fluid and fluid from the invaded zone. It allows calculating the contamination level and estimating the time required at a certain flow rate to reach a target contamination. The availability of GOR as part of formation testing proofed to be useful beyond the estimation of sample contamination. Mullins et al. (2001) present a comparison between laboratory GOR measurements and GOR derived from DFA measurements.

Fujisawa et al. (2003) present a technique of inferring five composition groups (C1, C2-C5, C6+, CO2 and water) from the near infrared absorption. The initial results show agreement with the mass fraction from laboratory analysis within +/- 5% accuracy for experiments conducted under elevated pressure and temperature. A field case is also presented.

Measuring fluorescence of condensate as it is subjected to a change in pressure helps to identify if it is undergoing a phase change. When the pressure drops below the dew point, liquid droplets form, which can be detected by a fluorescence sensor. Betancourt et al. (2004) introduce the sensor technology and discuss the application in field cases. The sensor is capable of detecting dew in concentrations as low as 1% vol (Betancourt et al. 2004).

Dong et al. (2008) introduce a new generation of DFA tool. It features an added 36 channel grating spectrometer for the range from 1600nm to 1800nm. A redesigned filter spectrometer still covers the range from 400nm to 2200nm. Additional sensors include a density and viscosity sensor, a resistivity sensor, a pressure and temperature gauge. The composition derived from the spectral response is extended by one more

group as compared with the previous compositional fluid analyzer: C1, C2, C3-C5, C6+ and CO2. Figure II.3 compares the composition measured by the laboratory and the composition measured with the new tool.

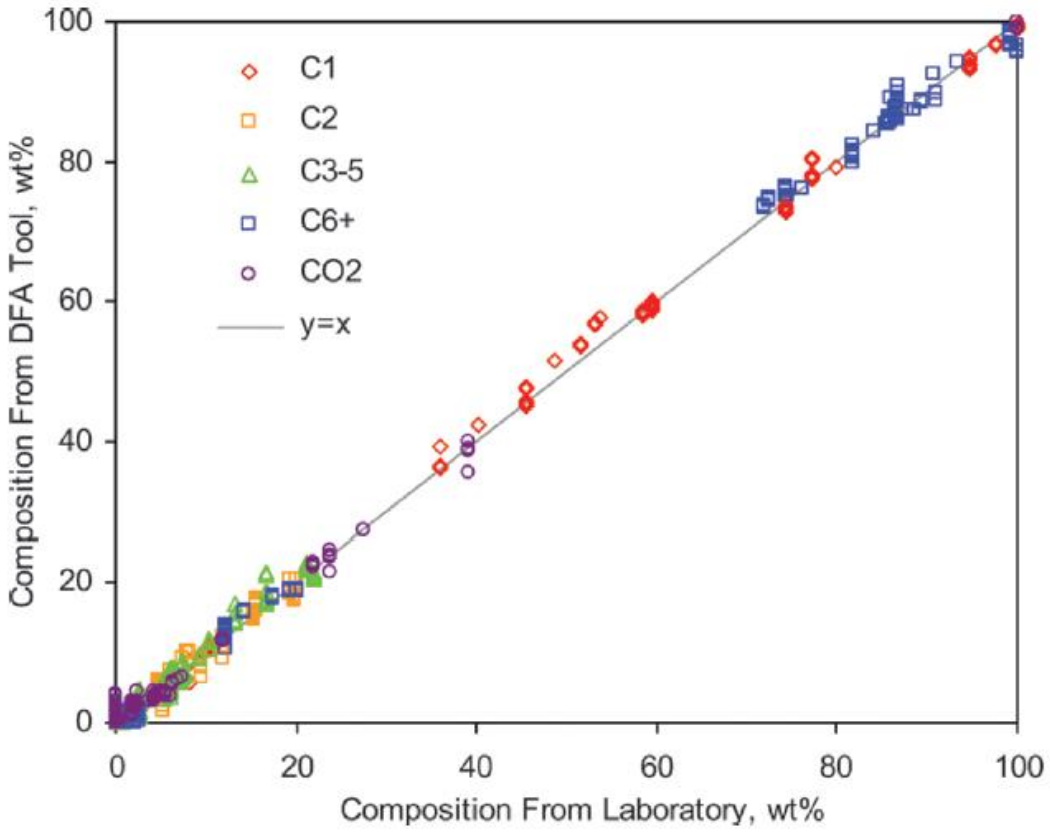

Figure II.3 – Comparison between composition from laboratory reports and the new DFA tool for various fluids (Dong et al. 2008).

Dong et al. (2008) present more graphs of the response of the various sensors. The test conditions are described and field studies are presented. Without giving hard numbers, the capability of conducting well to well comparison of the data is mentioned.

Mud filtrate contamination is always an issue when sampling or performing DFA in open hole. As an example, the difference between 2.6%wt oil based mud contamination and 19.4%wt contamination can make a difference of over 3000psi in the measurement of asphaltene onset pressure (O'Keefe et al. 2006). A technology that is capable of achieving zero percent contamination levels in open-hole sampling is focused sampling. O'Keefe et al. (2006) introduce the technology and report data from the first field test. The contamination of some of the samples acquired with the new technology is reported to be as low as 0.05%, 0.02% and 0%. Zero percent contamination means that the contamination is too low for the laboratory to measure it. A sample acquired for comparison with conventional technology under the same conditions with the same pumping time is reported to be 8.32% contaminated (O'Keefe et al. 2006). More case studies of the technique are presented by various authors (Contreiras et al. 2008; Weinheber and Vasques 2006; Weinheber et al. 2009). The technology can offer solutions in challenging sampling environments. A case of successfully sampling oil close to its saturation pressure in a well that was drilled through low permeability carbonate rock with oil based mud is an example of such a case (Contreiras et al. 2008). Cased-hole sampling or sampling during drill stem tests are alternatives to reach comparable contamination levels. The clear advantage of focused sampling is the availability of low contaminated fluid as early as during open hole logging operations. Therefore it links DFA into the early reservoir evaluation process at the time of exploration and appraisal drilling operations.

This chapter introduced DFA technology and gave an overview of the latest developments that enable accurate DFA. The reader is referred to the book by Mullins (2008) for further reading on the topic. The next chapter introduces the interpretation workflow. The prediction methods of fluid distributions, as outlined in Chapter III, allow distinguishing between equilibrium fluid columns and non-equilibrium conditions as soon as the data is acquired. The distinction between the two is integral to understanding fluid distributions and to constraining compartments using DFA data.

CHAPTER III

INTERPRETATION WORKFLOWS

Characterization of reservoir architecture is a complex task that involves earth scientists and engineers in multiple disciplines and roles. A thorough integration of all available resources, data and knowledge is needed to achieve a solid foundation for meaningful prediction of the field's performance. This is currently not common practice (Mullins 2008). A solidly built static reservoir model can be used to predict fluid columns. The prediction is then tested against the measurement and updated as the information becomes available. Once a static model stands and reflects the reality as it is measured in the field, it can be used to derive and simplify the dynamic model to simulate production. DFA is an integral part of this predictive workflow. An example of its use is the evaluation of the Tahiti reservoir in the Gulf of Mexico (Betancourt et al. 2007). The advantage in this case is that the DFA prediction model is adjusted while the DFA tool is still in the well. Based on the tuned model, the DFA data suggested compartmentalization even though the pressure gradient showed a continuous gradient within the sands. Subsequent analysis included reprocessing of the seismic data. A fault was detected by advanced fault detection algorithms and the compartmentalization was later confirmed by the production data (Mullins 2008). This example highlights the value and the need of an integrated approach.

Reservoir Charging and Mixing

Understanding reservoir architecture starts with understanding the elements and processes of the petroleum system. The work of Stainforth (2004) is summarized herein as it highlights some of the most relevant aspects.

Stainforth tests two end member hypotheses for trap filling. One assumes perfect mixing of the fluid in the trap and one assumes no mixing at all. Stainforth modeled the processes and compared the results under consideration of a variety of complexities. He found that in the majority of cases the later assumption matches reality.

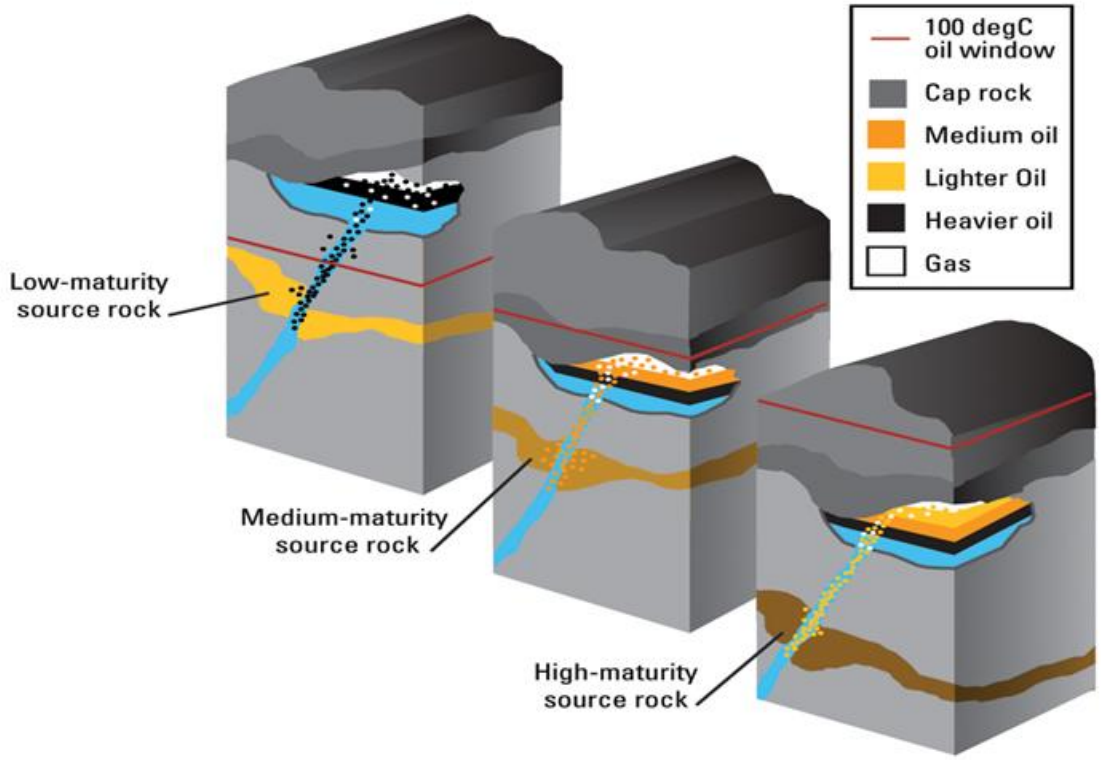

Figure III.1 – Charge history of a reservoir. The fluids layer into the trap in the order they arrive from the source rock (Stainforth 2004). Graphic from (Mullins 2008).

Perfect mixing of the fluids in the trap rarely occurs. That means that the fluids get layered into the trap in the sequence they arrive from the source rock. Figure III.1 visualizes this schematically. In a stacked reservoir the bottom trap fills first. Petroleum then migrates into the next pool by means of high permeability streaks like faults and other path ways. Hydraulic leakage may occur at the crest of the trap or the petroleum may spill into the next pool as it reaches capacity. As the kerogen becomes mature, it liberates lighter fluids. Lighter fluid displaces the heavier fluid in the trap from the top down as buoyancy forces drive this piston like displacement. According to Stainforth the API gravity reflects the maturity of the source rock. The gas oil ratio GOR and saturation pressure reflects the pressure and temperature history of the trap. The history of the source rock is not necessarily the same as the history of the trap. A variety of possible combinations lead to even larger varieties of API and GOR gradients (Stainforth 2004).

When working with DFA data it is important to understand the distances and length scales that govern reservoir mixing processes. Figure III.2 visualizes two schematic reservoirs.

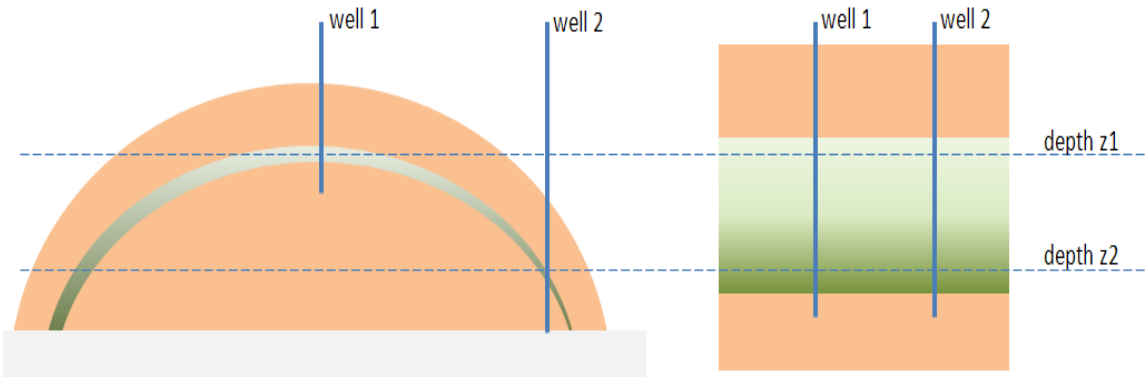

Figure III.2 – Two schematic reservoirs. A depth difference relates differently to lateral distances depending on the geologic structure of the reservoir. The distance over which the gas needs to diffuse into the oil column is higher in the reservoir on the left than in the reservoir on the right.

A depth difference relates differently to lateral distances depending on the geologic structure of the reservoir. In a reservoir of little vertical thickness, the fluid needs to equilibrate over large lateral distances, whereas in a reservoir of large thickness it is more likely that diffusion reaches equilibrium over geologic time (England et al. 1995).

Formation Pressure Surveys

When wireline formation testing is used, the quest for understanding reservoir architecture usually begins with a formation pressure survey. Pressure gradient analysis in a single or in multiple wells plays an important role in reservoir characterization. Even subtle discontinuities and differences in pressure gradients can indicate reservoir compartmentalization (Canas et al. 2008; Elshahawi et al. 2005; Jackson et al. 2007).

When studying pressure data, it is important to understand the accuracies and limitations of the pressure gauge as well as the depth measurement. The depth measurement in wireline formation testing can be affected by all aspects of depth control practices and depth measurement equipment. Ways to improve the accuracy of the depth measurements are discussed by Fitzgerald and Pedersen (2007). Less controllable are phenomena like tool creep. Tool creep refers to the movement of a wireline tool down hole after the winch has been stopped at surface. Practical methods to quantify tool creep are discussed by Fitzgerald (2008). With the technology and tools at hand all efforts shall be made to minimize the uncertainty in depth measurement. In any case a consistent approach throughout the data acquisition is recommended.

The accuracy and repeatability of the latest pressure gauges have improved, yet naturally there are statistical errors and limitations attached to the pressure measurement. For formation fluids of low densities, like gases and condensates, the limitations of the sensor technology may become an issue. Kabir and Pop (2007) discuss this subject, present case studies and outline methods to quantify the accuracy of the pressure survey. The authors show how the number of pressure measurements in a certain depth interval and the size of the interval itself affect the accuracy of the gradient. They present charts that may be used to decide on how many pressure measurements are necessary to obtain a meaningful gradient. Hashem et al. (2004) present further techniques to improve data quality of formation testing.

Formation pressure gradient analysis is a common practice. No one doubts its usefulness for fluid typing and compartmentalization evaluation. Pressure equilibration

occurs relatively quickly in comparison to the age of the reservoir and can happen across flow barriers (Muggeridge and Smalley 2008; Mullins 2008). Hence pressure communication is a necessary but insufficient condition for compartment connectivity.

If the gradient suggests a continuous pressure profile, compartmentalization can not be ruled out and further investigation using DFA is advised. The integration between DFA and pressure gradient analysis has been drawn by numerous authors (Dubost et al. 2007; Elshahawi et al. 2005; Montel et al. 2003; O'Keefe et al. 2007; Venkataramanan et al. 2006; Xian et al. 2010). In the MDT workflow, pressure analysis is still the first step to identify compartments. After this first step, DFA is applied to characterize the fluid content in the zones that were previously identified by the pressure analysis. Some parts of the reservoir may appear to be connected based on the pressure data. DFA helps to establish if they are in flow communication.

Fluid Comparison Algorithm

Compared to pressure gradients (generally interpreted as straight lines) the change in composition with depth is not as easily predicted. At the beginning DFA technologists evaluated how different the fluid is in different parts of the reservoir. As technology and understanding of DFA evolved, more refined approaches became available to predict and interpret DFA data in equilibrated columns.

Prior to the commercialization of the IFA attempts were made to systematically use the available DFA data to determine if two fluids are statistically different or similar. Venkataramanan et al. introduce a Fluid Comparison Algorithm FCA that takes

spectroscopic data from DFA and the level of contamination into account. Further inputs into the algorithm are the uncertainties and statistical errors of the measurement. This allows for example to quantify the effect of the use of different hardware. There are three possible outputs of the FCA: statistically similar, intermediate, statistically different (Venkataramanan et al. 2006).

Fluid property gradients can be vast enough to make two fluids appear statistically different even though they may be found in connected and equilibrated compartments. FCA reaches its limits in such highly graded columns. At the time when FCA was introduced, contamination was the main issue with DFA data. Focused sampling greatly reduces the influence of the drilling fluid contamination on the data. The accuracy of the data acquired with the latest generation DFA tool combined with a low level of contamination enables the use of EoS methods that supersede the methods of FCA (Zuo et al. 2008).

Integration of Equation of State Modeling and DFA

Integration of DFA measurements and modeling of fluid properties serves two primary purposes: It allows quality control of the data and a distinction can be made if the measurement indicates fluid equilibrium or not. EoS are widely used to estimate fluid properties of hydrocarbon mixtures of known composition. The motivation for modeling the fluid composition as a function of depth is to predict DFA data under the assumption of fluid equilibrium. If the measurement fails to match the prediction, the fluid may be out of equilibrium or the measurement is erroneous and needs to be

repeated. In either case, given that the control is done as soon as the data is acquired, further measurements can be done while the operations are still ongoing in the well.

DFA delivers compositional data in the form of weight percentages of the several component groups: CO2, C1, C2, C3-C5 and C6+. The tool infers fluid composition from a model. The input of the model is the spectroscopy data. Zuo et al. (2008) describe how the model is based on 103 different fluid samples ranging from heavy oil, black oil, volatile oil, gas condensate to wet gas. The samples were used to characterize the response of the tool at elevated pressure and temperature. The composition derived from the model is extended and grouped into pseudo components up to C30+. The model has then been tested with over 1000 fluid samples against composition from a gas chromatograph. The average absolute deviation (AAD) of the GOR prediction is 4.81% for a total of 1314 samples with an average deviation (bias) of 1.41%. For the prediction of the live fluid density the AAD is 2.49% and the bias is 0.37% (under consideration of more than 500 fluid samples). The developed technique allows using EoS calculations to predict the tool response at a different pressure and temperature (Zuo et al. 2008).

To improve the quality of the prediction, EoS are usually tuned to experimental data. The fluid measured by DFA naturally lacks experimental data in form of a laboratory report for tuning the EoS model. Zuo et al. (2009b) propose a workflow for integrating DFA station measurements with the EoS predictions. The first DFA station serves as a reference to build up the EoS model. The second station is used to tune the model by matching the data from both stations. The fluid profile can then be predicted. The data is matched by applying the Peneloux volume shift (Péneloux et al. 1982).

The prediction assumes a continuous column of equilibrated fluid. If one of the subsequent DFA stations produces data that does not match the prediction, at least one of these assumptions may not hold. The fluid at this point in the reservoir may not in flow communication with the previously measured fluid. In other words the fluid column is discontinuous. The second possibility is that the fluid is not fully equilibrated. In either case further investigation of the matter is advised. Ideally the tool is still in the well and the user can take full advantage of the real-time opportunity of this approach.

In the case that the data matches the prediction, it confirms the continuity of the reservoir fluid column and it can be used to further update and refine the predictive model. Figure III.3 shows a visualization of the steps and decisions that are necessary making use to the predictive EoS model.

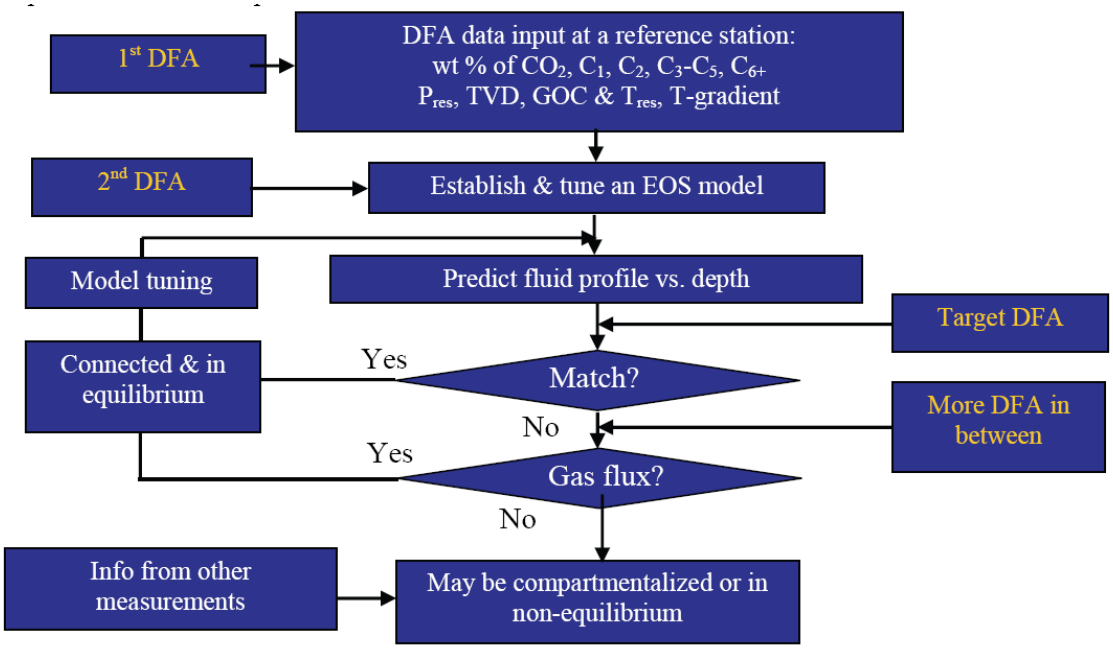

Figure III.3 – The work flow of EoS prediction of DFA data (Xian et al. 2010).

Modeling of Asphaltene Gradients

The low gas content gives low GOR oils or black oils a homogeneous character. It is this homogeneity that makes the use of black oil correlations possible and popular. In compressible fluids, the light components will cause greater expansion at shallower depth and thus give rise to GOR gradients. In incompressible fluids the density does not vary with depth, and thus there is no drive to create GOR gradients (Hoier and Whitson 2001).

When using fluid gradients to constrain compartments, homogeneity is counterproductive. However, black oils, even when found uniform in GOR, can still allow for asphaltene gradients (Mullins et al. 2010). These gradients can be measured by DFA. The color of a crude oil, as defined in the context of DFA, is closely linked to its

asphaltene content. A thorough understanding of asphaltene gradients is imperative - not only in the context of reservoir architecture, but also for a number of aspects of the petroleum production system (Mullins 2008). Understanding asphaltene gradients means the ability to model the asphaltene concentration with depth. This ability, will allow distinguishing equilibrium distributions from non-equilibrium fluid columns. An equilibrium distribution is a strong indication for possible connectivity throughout the reservoir (Zuo et al. 2009a).

How to model asphaltene gradients? EoS are developed to calculate gas-liquid equilibria. Critical properties of the components and acentric factors are the input to an EoS. Asphalteses, a solid matter, do not have critical properties. Any modeling of asphaltenes with an EoS is not proper. It has been done in the past, due to lack of alternatives. This approach is certainly not appropriate to predict gradients in a precise manner. Recently an alternative has become available (Zuo et al. 2010).

New advances in asphaltene science have made proper modeling of asphaltene gradients possible. The foundation of this advance is an understanding of the size and structure of asphaltene particles. The size and structure of asphaltenes is governed by the modified Yen model (see Figure III.4). The modified yen model distinguishes between asphaltene molecules, nano-aggregates and clusters of nano-aggregates (Mullins 2010a).

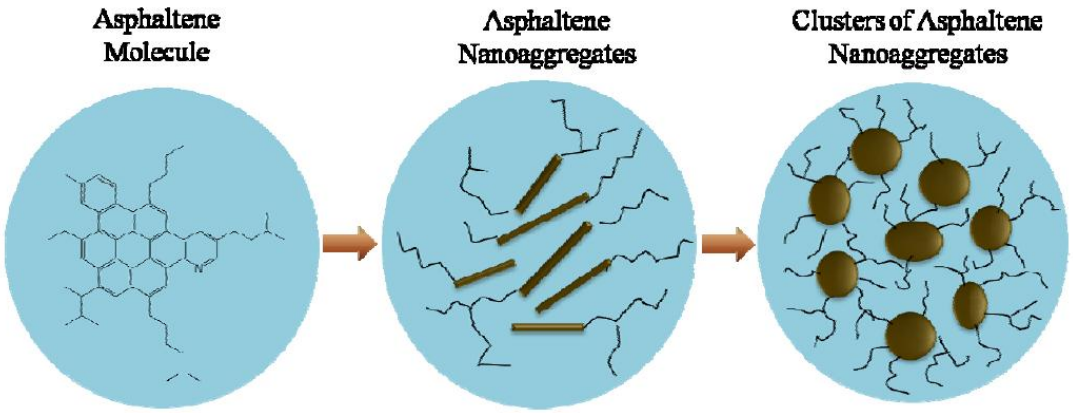

Figure III.4 – The modified Yen model (Mullins, 2010a). Asphaltene molecules have a molar mass of approximately 750 g/mole, nano-aggregates consist of approx. six molecules, clusters have about 8 nano-aggregates.

It specifies the amount of molecules in each species and accounts for size and mass. Knowledge of the molecular and colloidal properties of asphaltene is crucial to handle gravity effects. Other terms that govern the concentration of asphaltenes in crude oil are its solubility and entropy (Freed et al. 2010). The thermodynamic model proposed by Freed et al. develops these terms explicitly. It splits the crude oil in two components: Asphaltenes and the rest of the oil which are referred to as maltene. The change of properties with depth are modeled by an EoS. The properties of the asphaltenes are, in first approach, treated as constant with depth. If needed variations of the colloidal state with depth can be incorporated in the model. The solubility term of the model is heavily influenced by the GOR of the oil. For large GOR gradients the asphaltene gradient is dominated by the solubility of the crude oil. This effect is further illustrated in the first case study in Chapter V. In small GOR gradients gravity can be dominating. The EoS modeling as described earlier in this chapter can be used to model the properties of the

maltene. This approach firmly integrates DFA and asphaltene gradient prediction (Zuo et al. 2009a).

An equilibrated fluid column is a strong indicator for connectivity within the reservoir. The fact that the fluid has been in place for “geologic time” does not guarantee an equilibrated fluid column. England et al. were the first to point out that reservoir fluid mixing processes can exceed the typical age of a reservoir (England et al. 1987). A deviation from the equilibrated case does not automatically mean compartmentalization. The models and methods described above distinguish between equilibrium and non-equilibrium in real time. Parts of the reservoir that exhibit non-equilibrium need to be studied further and more data can be collected. Further interpretation of geological, geophysical and pertophysical data can be focused on that area of interest. Finally the most likely answer to the question of connectivity is derived from all information available.

In this chapter we have discussed the current state of the art of DFA data interpretation and its use in identifying compartments. The models and workflows presented assume the fluid is in equilibrium. The behavior of fluid composition in non-equilibrated columns is the main motivation for the simulation model that is introduced in Chapter IV.

CHAPTER IV

NON-EQUILIBRIUM MODELING

Many fluid columns that are investigated by DFA are found to be in thermodynamic equilibrium. Methods and processes exist to model the compositional gradients of such fluid columns. Chapter III pointed out that DFA data that deviates from the predicted composition may be indicative of compartmentalization. Another reason for the data to be poorly predicted by the EoS model is that the fluid has not reached equilibrium yet. A distinction between the two cases is necessary to identify compartments from DFA data. Both cases are complex and the reasons for a fluid column to be out of equilibrium are plentiful. Biodegradation, multiple and active charges, seal breaches, water washing, are examples of a school of processes that may cause the fluid to be in disequilibrium (Mullins 2008). Lateral diffusion across long distances in a reservoir is a slow process that may still be in a transient state when the reservoir is discovered (England et al. 1987).

The mass fluxes as described in Chapter III will try to equilibrate the fluid column. They are based on a chemical, gravitational, thermal and pressure potential. In most reservoirs the natural thermal gradient is too small to cause thermal convection. The critical Rayleigh number, a measure of the ratio of buoyancy forces and the product of thermal and momentum diffusivities, is not exceeded (England et al. 1995). Pressure diffusion equilibrates fast and does not need flow communication to reach equilibrium. Its effect on equilibrating the column is limited. The amount of flux required to equilibrate pressure is depending on the compressibility of the fluid. The lower the

compressibility, the smaller the amount of fluid that is required equilibrate pressure across the barrier. In an idealized case, two constant volumes filled with an incompressible fluid are considered, each one at a different pressure. An infinite small amount of fluid flow between the volumes is enough to equilibrate the pressure.

After the effects of pressure and thermal convection are considered as less important in the process of reservoir mixing, gravitational overturning and diffusive mixing remain. Diffusive mixing is a slow process, yet it is capable of moving substantial amounts of the fluid content in the reservoir. The amount of flux involved compared to pressure equilibration is large. This assumption is the foundation of using fluid gradients to constrain reservoir architecture. Figure IV.1 visualizes the amount of flux required for different processes in the reservoir.

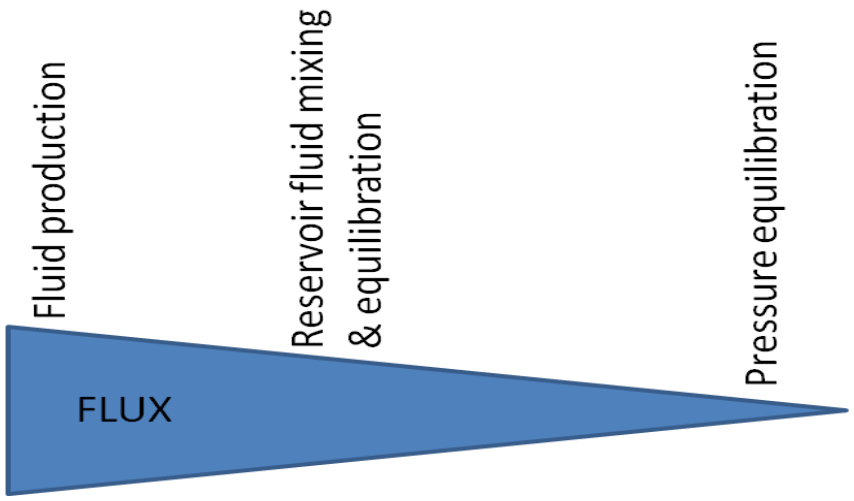

Figure IV.1 – The amount of flux required for different processes in the reservoir. Equilibration and fluid mixing processes require a substantial amount of flux compared to pressure equilibration.

A rigorous treatment of reservoir fluid modeling requires complex multi-component molecular diffusion of all the components in the mixture. In this study, the focus is to simulate diffusive mixing processes under reservoir conditions in order to understand the origin of large, non-equilibrium fluid gradients and the influence of fault transmissivity on these gradients. A simple diffusion model using activity-corrected component diffusion is investigated in this study using ECLIPSE* compositional simulator.

Introduction of the Simulation Model

In this nascent reservoir simulation approach, the idea is to first populate the model with pressure and multi-component fluids distribution in a manner that represents the initial hydrocarbon charge into the reservoir and then to allow reservoir fluid mixing to evolve over time mainly under diffusion. This is a slow process which involves geological time-scales. Reservoir simulators are designed to make predictions of production and its use to simulate processes over millions of years is rare. This fact leads to the desire to test the simulator in a variety of cases to evaluate its sensitivity to parameters like gridblock size, number of gridblocks, overall grid dimensions, range of diffusion coefficients etc. In order to concentrate purely on the effects of molecular diffusion these sensitivities have been evaluated in a variety of 1D horizontal model simulations.

All models in these sensitivity trials share some common properties. The model consists of a horizontal string of gridblocks under isothermal condition. The gridblock dimensions are 100m in z and y direction. The dimension in the x direction may vary

depending on the case. The depth of the top of the model is set arbitrarily to 2100m. The porosity is 20% and permeability is 1000mD. The relative permeability curve is shown in Figure IV.2. The fluid used in these first sensitivity runs is designed to remain as a single phase liquid. Thus relative permeability will have no effect here, however multiphase cases will make use of these curves later. Capillary pressure effects are not considered.

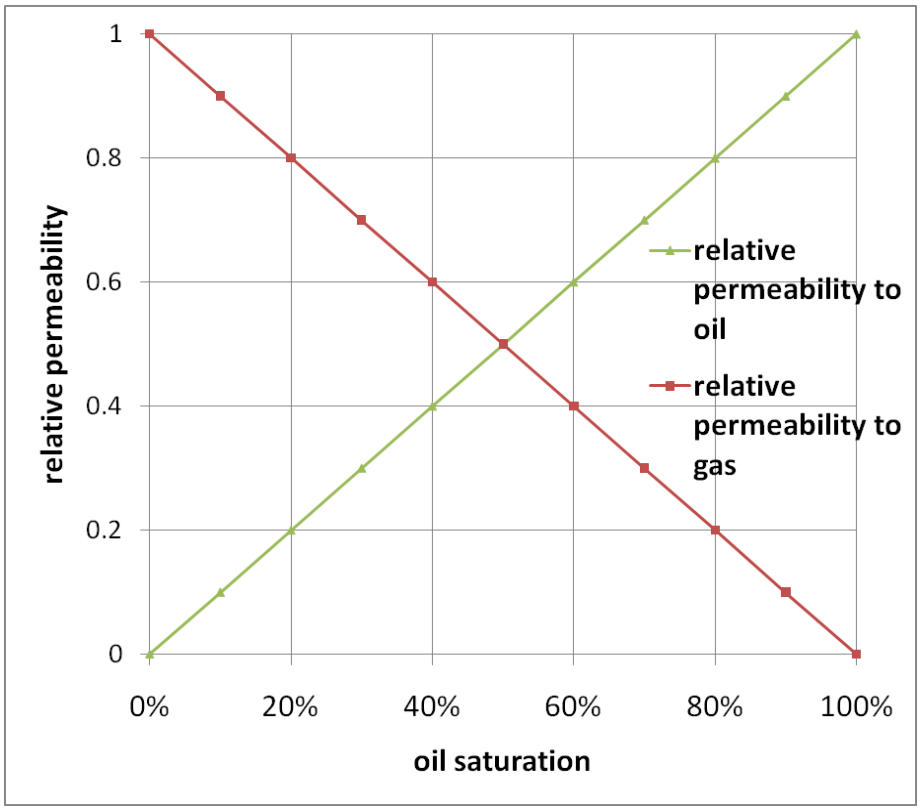

Figure IV.2 – Relative permeability curves of the simulation model.

Figure IV.3 shows a visualization of an example case. The model is initialized with two binary mixtures with different concentrations of C1 and C2+. The two mixtures

only differ in their composition. This difference in the split between the two components in each half of the model is creating the necessary chemical potential for diffusion to take place. Table IV.1 shows the split between the two components and how they are initially distributed in a model of 100 gridblocks.

Table IV.1 – Initial fluid distribution

	grid 1-50	grid 51-100
C1 mole fraction	0.28	0.2
C2+ mole fraction	0.72	0.8

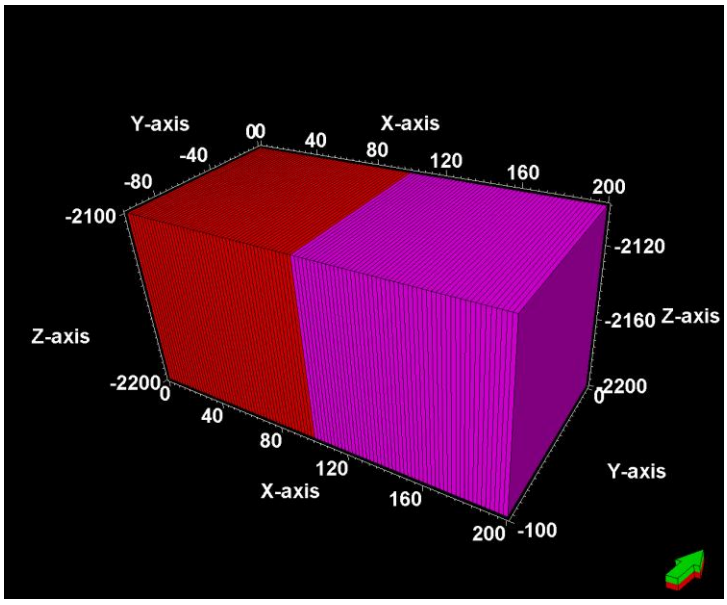

Figure IV.3 – Example of horizontal 1D simulation model.

Albert Einstein related the mean square displacement R^2 of a particle under Brownian motion to the product of its molecular diffusion constant D and the diffusion time t:

$$R^2 \sim D * t; \tag{IV.1}$$

The average distance that the molecules have to travel to equilibrate the model is affected by the overall dimensions, the initial distribution, tortuosity and other scaling factors for diffusion length in a porous medium. Einstein's simple relation is put to use to find a criterion to compare the different scenarios of model length and diffusion constants. The criterion $\sqrt{D * t}/L$ is expected to be constant for all cases, with L being the half-length of the model. Even though the gridblocks have a dimension of 100m in the z direction, changes are only calculated between gridblocks. The properties within one gridblock are assumed to be constant. Hence gravity effects can be neglected in a one-dimensional horizontal model.

During the simulation the change of the mole fraction of the two components in a representative amount of gridblocks is monitored. The component is considered equilibrated when its mole fraction is uniform in all sample gridblocks.

The diffusion coefficients have a scaling effect on the equilibration times. The sensitivity of the model towards the choice of coefficients is part of the testing of the model. The diffusion coefficients assigned to the two components are arbitrarily chosen and then varied by an order of magnitude up and down. A method of estimating the diffusion coefficients of hydrocarbon components under reservoir conditions will be

shown later in this chapter. The three sets of coefficients, labeled regular, fast and slow, that were used for this sensitivity study are shown in Table IV.2.

Table IV.2 – Three sets of diffusion coefficients for a binary mixture

	regular	fast	slow
D1 – diff. coeff. of C1 [m^2/day]	1.20E-04	1.20E-03	1.20E-05
D2 – diff. coeff. of C2+ [m^2/day]	2.80E-04	2.80E-03	2.80E-05

A number of 21 simulation runs were performed using a model with a constant number of 100 gridblocks. For each set of diffusion coefficients the dimensions of the gridblocks were varied to obtain a model half-length of 10m, 50m, 100m, 500m, 1000m, 5000m, 10000m. Table IV.3 a-c show the results of these simulation runs.

Table IV.3 – Equilibration times for different model half-lengths. The ratio of Einstein's mean square displacement to the half-length is constant

a) Regular set of diffusion coefficients

Model half-length [m]	C1 equilibration time [years]	C2+ equilibration time [years]	SQRT(D1*t1)/L	SQRT(D2*t2)/L
10	1.11E+04	9.90E+03	0.17649	0.10901
50	2.58E+05	2.30E+05	0.16987	0.10514
100	9.13E+05	8.16E+05	0.15993	0.09895
500	2.47E+07	2.22E+07	0.16644	0.10331
1000	9.42E+07	8.42E+07	0.16239	0.10051
5000	2.46E+09	2.06E+09	0.16594	0.09941
10000	8.91E+09	8.11E+09	0.15799	0.09868

b) Fast set of diffusion coefficients

Model half-length [m]	C1 equilibration time [years]	C2+ equilibration time [years]	SQRT(D1*t1)/L	SQRT(D2*t2)/L
10	9.15E+02	8.19E+02	0.16009	0.09913
50	2.24E+04	2.00E+04	0.15849	0.09804
100	8.62E+04	7.97E+04	0.15535	0.09779
500	2.31E+06	2.08E+06	0.16089	0.09985
1000	9.03E+06	8.09E+06	0.15897	0.09852
5000	2.24E+08	1.99E+08	0.15843	0.09776
10000	8.98E+08	8.01E+08	0.15860	0.09804

Table IV.3 Continued
c) Slow set of diffusion coefficients

Model half-length [m]	C1 equilibration time [years]	C2+ equilibration time [years]	SQRT(D1*t1)/L	SQRT(D2*t2)/L
10	9.22E+04	8.25E+04	0.16070	0.09948
50	2.26E+06	2.02E+06	0.15897	0.09852
100	9.37E+06	8.37E+06	0.16196	0.10022
500	2.35E+08	2.10E+08	0.16227	0.10042
1000	9.00E+08	8.05E+08	0.15871	0.09827
5000	2.20E+10	1.98E+10	0.15695	0.09738
10000	7.89E+10	7.81E+10	0.14865	0.09682

During the study it was found that large time steps can distort the results. A small enough time step granularity is needed to adequately capture the correct equilibration time.

Another sensitivity study varied the number of gridblocks for a variety of different model half-lengths. This was done to further test the simulators robustness against the model's geometry. A total of 18 cases were run for three different model half-lengths of 500m, 5000m and 10000m with the following numbers of gridblocks: 10, 50, 100, 200, 500, 1000. It can be seen from the equilibration times in Table IV.4. a-c, the simulation results are very consistent.

Table IV.4 – Equilibration times for models of constant half-length made up by a varying amount of gridblocks. The equilibration time and the ratio of Einstein's mean square displacement to the half-length remains constant.
a) Model half-length 10000m

Model half-length [m]	C1 equilibration time [years]	C2+ equilibration time [years]	SQRT(D1*t1)/L	SQRT(D2*t2)/L	number of grid blocks n
10000	9.05E+09	7.93E+09	0.15919	0.09756	10
10000	9.05E+09	7.93E+09	0.15919	0.09756	50
10000	9.05E+09	7.93E+09	0.15919	0.09756	100
10000	9.05E+09	7.93E+09	0.15919	0.09756	200
10000	9.05E+09	7.93E+09	0.15919	0.09756	500
10000	9.05E+09	7.93E+09	0.15919	0.09756	1000

b) Model half-length 5000m

Model half-length [m]	C1 equilibration time [years]	C2+ equilibration time [years]	SQRT(D1*t1)/L	SQRT(D2*t2)/L	number of grid blocks n
5000	2.4E+09	2.2E+09	0.16343	0.10334	10
5000	2.4E+09	2.2E+09	0.16343	0.10334	50
5000	2.4E+09	2.2E+09	0.16343	0.10334	100
5000	2.4E+09	2.2E+09	0.16343	0.10334	200
5000	2.4E+09	2.2E+09	0.16343	0.10334	500
5000	2.4E+09	2.2E+09	0.16343	0.10334	1000

Table IV.4 Continued
b) Model half-length 5000m

Model half-length [m]	C1 equilibration time [years]	C2+ equilibration time [years]	SQRT(D1*t1)/L	SQRT(D2*t2)/L	number of grid blocks n
500	2.6E+07	2.3E+07	0.17018	0.10589	10.0
500	2.6E+07	2.3E+07	0.17018	0.10475	50.0
500	2.6E+07	2.3E+07	0.17018	0.10475	100.0
500	2.6E+07	2.3E+07	0.17018	0.10475	200.0
500	2.6E+07	2.3E+07	0.17018	0.10475	500.0
500	2.6E+07	2.3E+07	0.17018	0.10475	1000.0

A sensitivity study of the influence of porosity on the diffusive equilibration time shows little to no influence of the porosity as long as it is kept uniformly throughout the model. A baffle consisting of two gridblocks with a porosity of 1% is then introduced in the middle of a model with otherwise uniform porosity of 20%. As a result the equilibration time almost doubles. These results are shown in Table IV.5. This is in line with the calculation of the diffusivity between adjunct cells in ECLIPSE*. As porosity changes from one cell to another, some of the pores will dead-end at the seam between two gridblocks. The result is a reduction in diffusivity.

Table IV.5 – Influence of porosity on equilibration times. When applied uniformly, the influence of porosity on equilibration times in the model is little to none. A non uniform porosity distribution (last row) – here in form of a two gridblock wide baffle – impacts the equilibration time

Model half-length [m]	C1 equilibration time [years]	C2+ equilibration time [years]	SQRT(D1*t1)/L	SQRT(D2*t2)/L	porosity
100	9.13E+05	8.16E+05	0.15993	0.09895	20.00%
100	9.13E+05	8.16E+05	0.15993	0.09895	10.00%
100	9.13E+05	8.16E+05	0.15993	0.09895	5.00%
100	9.13E+05	8.16E+05	0.15993	0.09895	1.00%
100	9.13E+05	8.16E+05	0.15993	0.09895	0.10%
100	9.10E+05	8.16E+05	0.15959	0.09895	0.01%
100	1.63E+06	1.46E+06	0.21375	0.13218	20% with two-cell 1% porosity baffle

As in the porosity case above, a uniform change in permeability does not affect the equilibration time. Then a permeability baffle is introduced: the middle two cells in the model are assigned a low permeability. The porosity is kept constant throughout at 20%. Surprisingly this baffle does not influence the equilibration time.

In ECLIPSE* the permeability only affects the transmissivity between two cells. The permeability and transmissivity will affect for example the flow of fluid in the model towards a well. For diffusive flux however, transmissivity and permeability are not taken into account. In ECLIPSE* only the diffusivity is relevant for the diffusive flux. Table IV.6 shows the simulation results that cover the permeability sensitivity.

Table IV.6 - Influence of permeability on equilibration times. The equilibration times in the model change little to none, even when the permeability is applied non uniformly (last row). In ECLIPSE*, permeability influences transmissivity. Diffusivity – the measure that affects equilibration time and diffusive flux- is not affected by permeability changes

diffusion Length L [m]	C1 equilibration time [years]	C2+ equilibration time [years]	SQRT(D1*t1) /L	SQRT(D2*t2) /L	horizontal Permeability [mD]
100	9.13E+05	8.16E+05	0.15993	0.09895	100.00
100	9.13E+05	8.16E+05	0.15993	0.09895	10.00
100	9.13E+05	8.16E+05	0.15993	0.09895	1.00
100	9.13E+05	8.16E+05	0.15993	0.09895	0.10
100	9.10E+05	8.16E+05	0.15959	0.09895	0.01
100	9.21E+05	8.12E+05	0.16061	0.09871	100 - with 0.01 two cell baffle

Component and fluid flux is essential for fluid redistribution and reservoir mixing. Large volumes have to redistribute, for the fluid column to equilibrate. This requires a fair amount of flux. Chemical potential is the driving force of diffusion. For a chemical potential to form fluids of different compositions need to be in contact with each other. As far as the simulation model is concerned, a reduction in contact area reduces the diffusivity between two adjunct cells. A reduction in porosity from one cell to another reduces the contact area, whereas a uniform reduction of porosity in all cells will reduce the overall amount of fluid that is considered, but will have no impact on the chemical potential.

The simulator treats transmissivity and diffusivity as separate, unrelated phenomena. A change only in permeability has no effect on the diffusive flux in the

simulation, if the porosity is left unchanged. In nature porosity and permeability rarely change in an unrelated manner. Even though there is no analytical relationship between porosity and permeability, the two properties are in most cases linked statistically.

If a closer representation of a specific case is desired, a more detailed look into the permeability-porosity relation of the field would be advised. Since only connected pores contribute to the diffusive flux an examination of effective porosity versus total porosity would also be necessary.

The effect of tortuosity on the actual diffusion length needs also be considered. Tortuosity accounts for the increased length through witch matter must diffuse in a porous medium as opposed to a straight line. England et al. (1987) suggests a value of ¯ for rock matrixes and refers to the work of Li and Gregory (1974). England also points out that large scale tortuosity effects may be present. Dykhuisen and Casey (1989) also suggest a value of ¯, but restrict it's applicability to homogeneous and isotropic rocks. In nature where pores vary in cross section and coordination number, tortuosity may well deviate from this value. Boving and Grathwohl (2001) show that tortuosity scales with absolute porosity:

$$\tau = \phi^{-1.2} \tag{IV.2}$$

They also introduce an effective diffusion coefficient that depends on effective porosity and tortuosity:

$$D_{eff} = D * \frac{\phi_{eff}}{\tau} \tag{IV.3}$$

Their work is based on a variety of different rock samples. The diffusion experiments are based on tracer migration in water filled rock samples under laboratory conditions.

Caution must be taken when findings of experiments on small rock samples are extrapolated on large scale rock formations (Boving and Grathwohl 2001).

Other factors might affect diffusion, but have not been taken in to account. The roughness of the pore wall, coordination number and porethroat size distribution comes to mind. One can imagine differential retention effects of the porous medium on the fluid similar to a chromatograph. Also the effect of dual porosity and fractures are not studied here.

Reasonable Choice of Diffusion Coefficients

The influence of the diffusion coefficients on the equilibration time is unquestioned. A representative choice of coefficients is not trivial. The Stokes-Einstein equation relates the diffusion coefficient inversely to the viscosity of the fluid. It is the base of many correlations including some described by Taylor and Krishna (1993). A well known reference in on this topic is also the book by Poling, Prausnitz and O'Connell (2001). More on the topic, with a focus on porous media is described by Grathwohl (1998). Most of the correlations that are widely used for surface conditions seem to fail for high pressure systems. Riazi and Whitson (2003) show that under high pressure the diffusion coefficients of some experimental correlations almost double. Liu and Macedo (1995) present a correlation aimed at a large range of pressure and temperature with good results. They limit their work to carbon dioxide, water, methane, ethane and deuterium. Jamialahmadi et al. (2006) use an experimental set up to estimate the diffusion coefficient of methane at reservoir conditions. Further examples of

estimating diffusion coefficients under reservoir conditions are found here: Grogan et al. (1988); Riazi (1996). All of these authors limit their work to one or a small subset of components found in petroleum fluids. The solute is assumed to be small in concentration compared to the solvent. For petroleum fluids found in the reservoir, this assumption does not hold. The diffusive flux of one component does not only depend on its own chemical gradient, but also on the chemical gradient of all other components present in the mixture. This is called mutual diffusion as opposed to self diffusion. Curtiss and Bird (1999) review the major formulations of diffusions in multi-component mixtures. When considering a mixture of petroleum fluid components, mutual diffusion would need to be considered to accurately represent the physics. Self diffusion coefficients for components in a binary mixture can be corrected using the Darken Equation (Darken 1948). Once more than two components are present the relationship between self diffusion and mutual diffusion becomes very complex. To the best of my knowledge no usable equations exist to relate the two.

Freed et al. (2005) aim their research at relating the nuclear resonance of a petroleum fluid to its composition. They found that the self diffusion coefficient of each component scales with its chain length in form of a power law (Freed 2007; Freed et al. 2005). Freed (2009) presents a method to apply a correction to the diffusion coefficients for elevated temperatures and pressures. Her method takes the mean chain length of the entire mixture into account. Thus it can be applied to any composition of petroleum reservoir fluid – gas or liquid. Her work is lacking any reference to non hydrocarbon components like nitrogen, carbon dioxide or hydrogen sulfide. It is a reasonable

assumption to assign diffusion coefficients of hydrocarbon components of similar molecular size to these non hydrocarbon components. This assumption is in good agreement with the results of Liu and Macedo (1995), mentioned above.

An example illustrates the concept of component chain length and average chain length of oil and gas. Each component is assigned a chain length N_i. The non-hydrocarbons are assigned the same chain length as a hydrocarbon of similar molecular size: Carbon dioxide is treated like propane and nitrogen is treated as methane. Freed found that for lighter components the diffusion coefficients follow a modified power law. The individual chain length is adjusted and the average chain length is replaced by +1. A personal conversation with Freed on how to assign the individual chain length to lighter components is summarized in Table IV.7.

Table IV.7 – Chain length assigned to light components. These values are used in the calculation of the corresponding diffusion coefficients

Component	Chain length N_i
Nitrogen	2
Methane	2
Ethane	3.3
Carbon Dioxide	3.3
Propane	4.2
I - Butane	4.8
N - Butane	4.8
I - Pentane	5.3
N - Pentane	5.3
C6	6

For all SCN groups of C6 and higher the assignment is straight forward: C6: $N_i = 6$; C7: $N_i = 7$; C29: $N_i = 29$. For the plus fraction C30+ a chain length of 30 is assumed. The average chain length for oil and gas can be calculated as a weighted average of the individual chain lengths. Each of the components individual chain length is weighted with their mole fraction. For oil this average includes the components from C6 to C30+, for gas the average is based on all light components C1-C5 and the non-hydrocarbons.
The diffusion coefficients are then calculated using:

$$D_i = A(p,T)N_i^{-\upsilon}\bar{N}^{\beta(p,T)}\,; \qquad \text{(IV.4)}$$

For details of the calculation of A(p, T), β(p, T) and ν the reader is referred to the original publication (Freed 2009).

ECLIPSE* gives a choice of two diffusion models: activity driven diffusion and molecular driven diffusion. In activity driven diffusion, mass transfer between cells is driven by the chemical potential. It allows diffusion over phase boundaries. The activity driven diffusion option is used throughout this work. This model allows for the input of two diffusion coefficients per component – one for each phase (liquid and gaseous). Mutual diffusion is not considered in ECLIPSE*. Throughout this work, self diffusion coefficients are assigned to the components in the liquid phase and in the gas phase. These coefficients have been corrected for temperature and pressure.

Freed's method is a workable choice for our purposes. To the best of my knowledge there is not any approach in the literature that offers an equal amount of practicality combined with the level of refinement. It is practical in the way it adapts to any fluid composition and it allows calculating coefficients for all components in the gas phase and the liquid phase in a consistent manner. Some amount of error is introduced by not taking into account the effect of mutual diffusion – a process that is not well understood to begin with.

Fluid Composition and Component Grouping

A compositional report of a real reservoir fluid contains a large amount of hydrocarbon and some non-hydrocarbon components. The total amount of components that can be specified in ECLIPSE* is limited to 40. Even though a simulation of a 40 component fluid is possible in a simple one dimensional model, the reservoir fluid can be adequately represented by a smaller number of pseudo components. Various models are available in the literature to calculate the properties of the pseudo components. Tuning procedures to for EoS calculations to match data from fluid samples are commonly in use.

Accurate tuning is necessary in simulations for purposes like reserve calculation, production prediction or any other aspects of simulation work that has to rely on accurately represented phase behavior of the fluid column. This work uses parts of the steps to tune an EoS. The simulations of this work use example compositions that may be altered for the purpose of sensitivity studies. There is an interest to use real fluid

compositions, yet a full tuning procedure is of little value when the compositions are purposely altered.

The work of Al-Meshari and McCain (2005) outlines a well structured step by step method to tune a EoS model to laboratory data. Al-Meshari, Aquilar-Zarita and McCain (2005) present compelling arguments for the use of this method. More on this method of splitting, grouping and tuning can be found here: Al-Meshari and McCain (2006, 2007). Also for practical reasons like the availability of Dr. McCain at the department this set of methods was selected to populate the simulation model with fluid data. Since the actual tuning is ignored, any other method found in the literature would lead to ultimately the same results.

The first step is to characterize the laboratory plus fraction. The intent is to use statistical methods to make an assumption of the composition of what has been reported as C7+, or C20+ or C36+ etc. After the plus fraction has been extended to a sufficient number of SCN components (up to SCN 45 is common), correlations are used to assign critical properties and acentric factors to the pseudo components. (Cavett 1962; Riazi and Al-Sahhaf 1996). A set of equations calculates the molefraction, critical properties and acentric factors for a set of pseudo components. Some pure components like methane, carbon dioxide, nitrogen and hydrogen sulfide will not be grouped.

Figure IV.4 show the original composition, Figure IV.5 the extended composition and Figure IV.6 the grouped composition of an example fluid. To facilitate the calculations, a programming code in Mathematica** was developed.

***Mathematica is a mark of Wolfram Research inc.*

Table IV.8 summarizes the critical properties and acentric factors of the pseudo component generated by the Mathematica** code, using the equations outlined by Al-Meshari and McCain (Al-Meshari and McCain 2005).

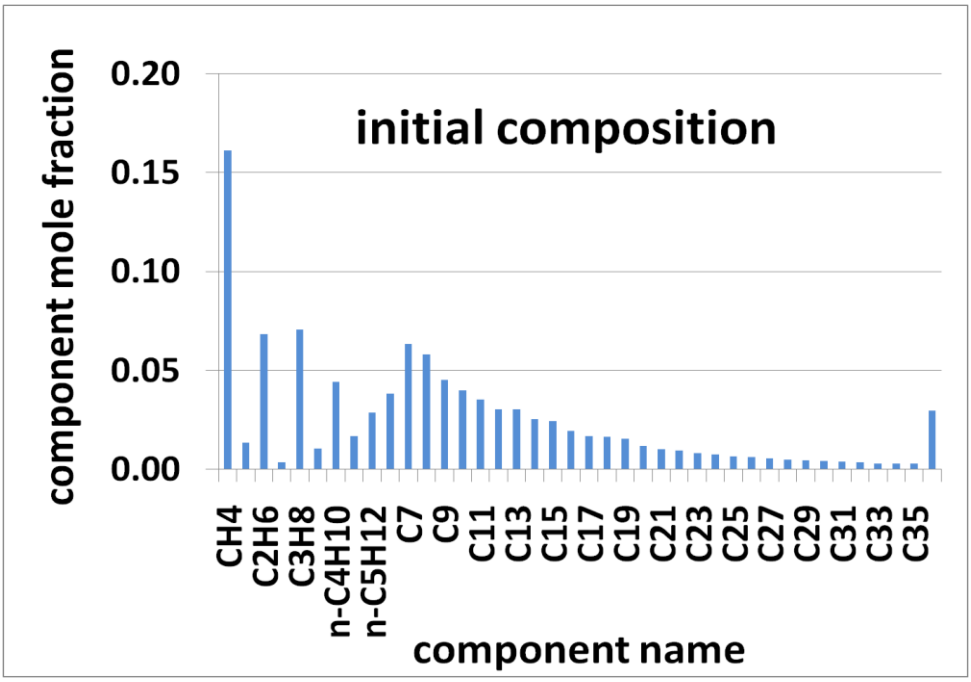

Figure IV.4 – Original composition of example fluid.

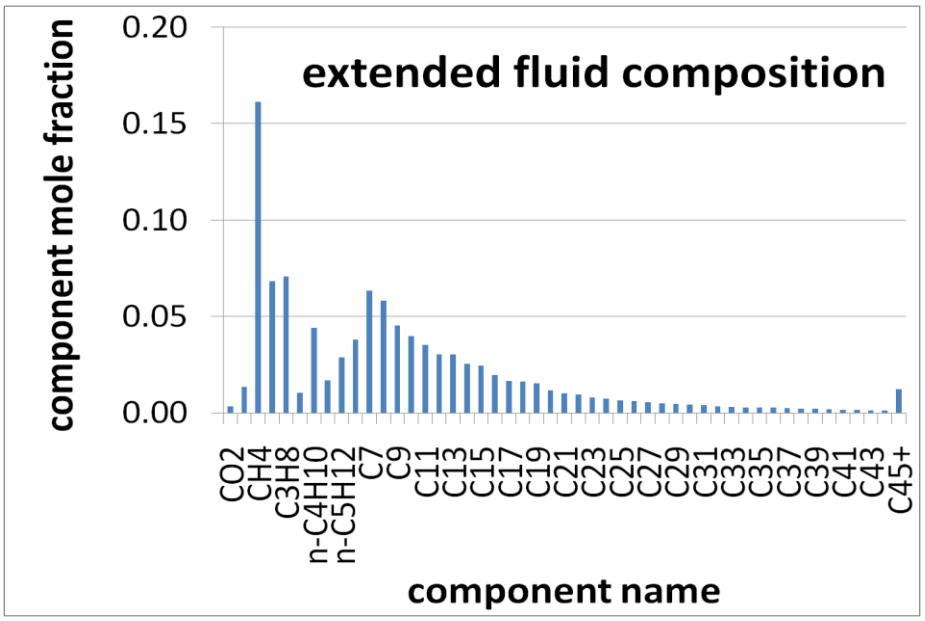

Figure IV.5 – Extended composition of example fluid. Components are represented by SCN groups up to C45+.

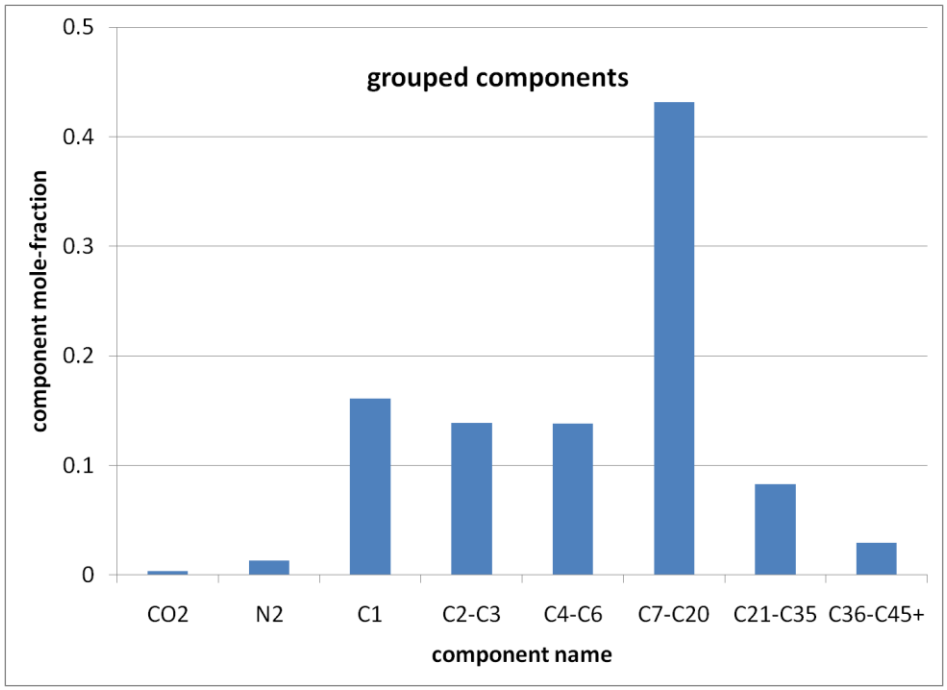

Figure IV.6 – Grouped composition of example fluid. This composition together with the properties of Table IV.9 are used in PVT-i to generate the fluid model keywords and data for ECLIPSE*.

Table IV.8 – Properties of pseudo components of example fluid

	mole fraction	critical pressure, psi	critical temperature, °R	acentric factor	apparent molecular weight, g/mole
carbon dioxide	0.0020	1070.7000	547.5000	0.2230	44.0100
nitrogen	0.0012	493.1000	226.8000	0.0400	28.0100
methane	0.3400	666.4000	343.0000	0.0104	16.0400
C2-C3	0.1102	652.0190	615.5420	0.1285	37.7646
C4-C6	0.1155	502.2707	838.6222	0.2332	71.2218
C7-C24	0.2946	285.0934	1213.0662	0.5648	174.0342
C25-C44	0.0861	148.0766	1645.3175	1.3168	465.8728
C45+	0.0505	149.1000	1940.0000	2.2247	878.2800

The data in Table IV.8 serves as input to the software PVT-i. PVT-i is then used to generate a set of ECLIPSE* keywords and values that specify the necessary fluid properties for the simulation. The mole fraction of carbon dioxide and nitrogen is low compared to the other components. If one was to decide not to keep track of these components they should be lumped together with a component of similar boiling point temperature.

CHAPTER V

CASE STUDIES

The design of a field development plan may present engineers and scientists with many challenges. Understanding the reservoir architecture is crucial for success. DFA can not give all the answers to these challenges. Yet if applied properly it can give the necessary leads to probe the model in the right way to finally get to the right answers. It is a tool that can prove to be very powerful in the hand of a skilled engineer. Awareness of nascent developments in DFA and the adjunct theory that describes fluid distributions is part of that skill. In this chapter two cases of field data are presented. One case will show how the application of the fluid simulation model of Chapter IV ties in with new theory of asphaltene science. It will help explain the origin of an extreme compositional gradient that previously was not well understood. A second field case revolves around a field in the Malay Basin. Its low GOR oil shows a large gradient of carbon dioxide. This example will show how the simulation may - when taken out of context - show results that can be interpreted in two very different ways. It reveals the importance of integrating knowledge about the geologic setting of the entire petroleum system into the interpretation of the data and simulations. It also shows how the right amount of DFA stations can largely improve the confidence towards understanding the architecture of this field.

The methods and simulations described in Chapter IV are aimed to understand and test the behavior of a simplified reservoir model. Transport processes, mainly diffusive flux, are simulated in a static, closed system. Those simulation models are

nowhere near a real reservoir model in any respect. Yet these models can achieve, in their simplicity, a plausible explanation for the origin of a fluid distribution. This will trigger further investigation and may justify more data acquisition. As a result, the hypothesis proposed by the simulation can be probed in a structured, well directed manner.

Case 1: Secondary Gas Charge

Elshahawi et al. describe a case of an oil column that exhibits an unusually large gradient in GOR over a relief of 400ft in the Gulf of Mexico. The disequilibrium is caused by a large influx of biogenic methane into a black oil column (Elshahawi et al. 2007). The changing carbon isotope ratio (δC13) across the field is proof of the disequilibrium. It also identifies the inflowing methane to be of biogenic origin. The gas accumulates updip (Elshahawi et al. 2007). The change of GOR and saturation pressure with depth is shown in Figure V.1

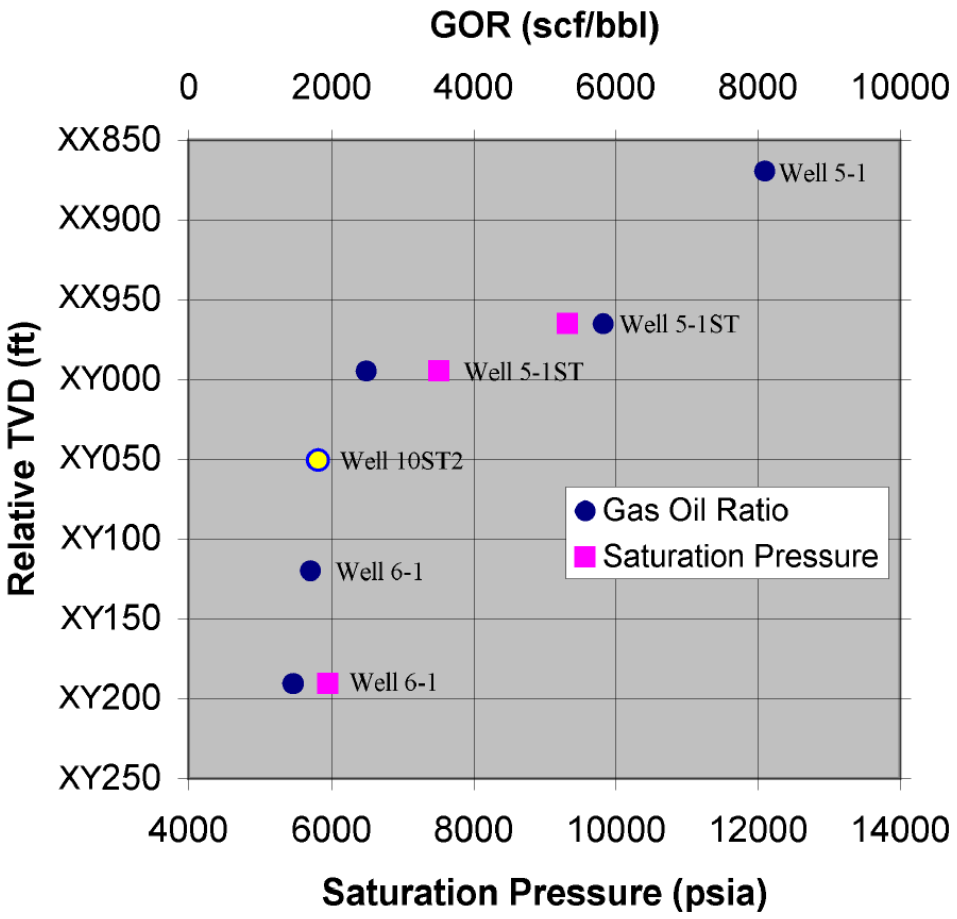

Figure V.1 – GOR and saturation pressure of a fluid column in disequilibrium (Elshahawi et al. 2007).

This large, non-equilibrium gradient of GOR and saturation pressure is a result of the late methane charge. The GOR gradient produces a huge gradient in the solubility parameter of the asphaltene model (see Chapter III). The large disequilibrium distribution of asphaltenes is shown in Figure V.2. It allows comparison of the data determined by DFA (bottom horizontal axis: color) and the laboratory (top horizontal axis: weight percent of asphaltenes). The gas influx destabilizes the asphaltenes at the top of the column. Nano-aggregates form clusters of nano-aggregates. Theses clusters

stay suspended in the mixture. The important fact is that they do not seek solid surfaces to stick to, like flocks of asphaltenes would do. Gravity pulls the clusters towards the bottom of the column.

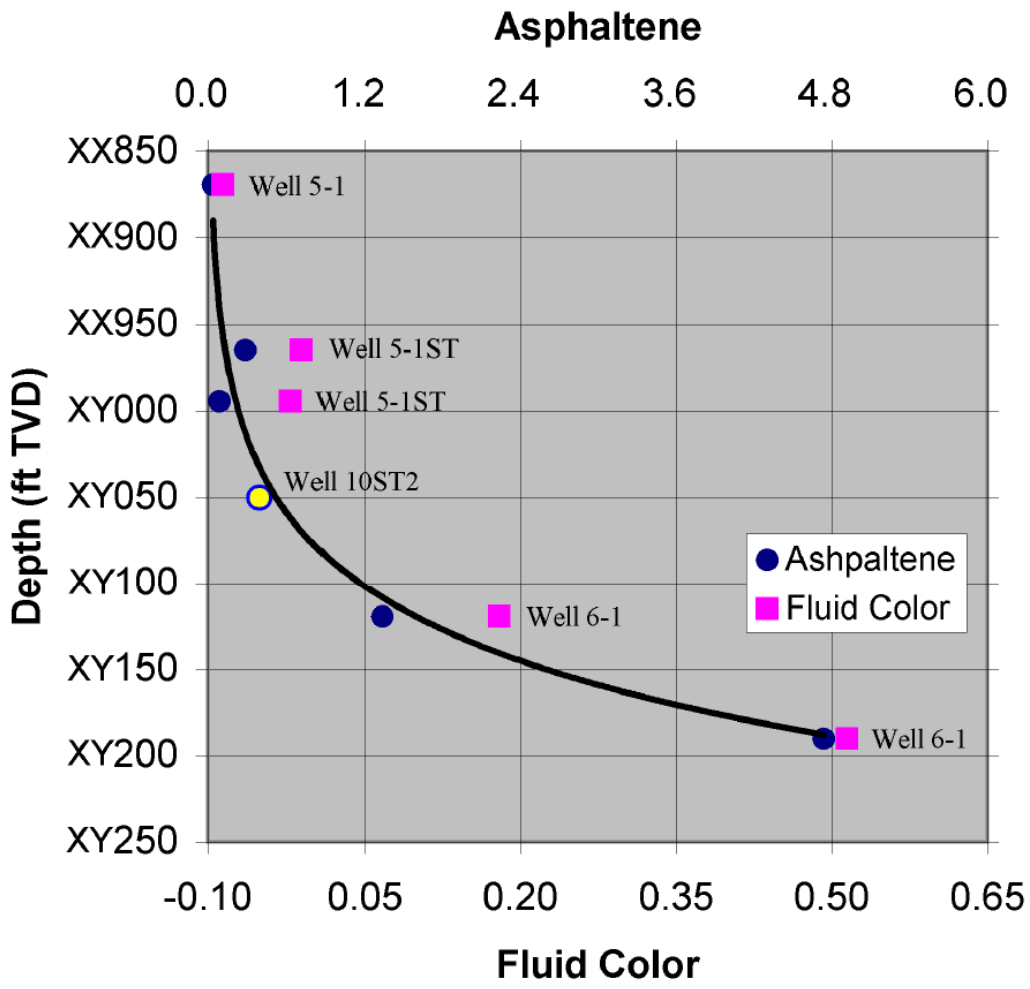

Figure V.2 – Large disequilibrium distribution of asphaltenes. Data determined by DFA: bottom horizontal axis – color. Data determined by the laboratory: top horizontal axis - wt%-asphaltene. The gradient is a result of gas induced instability of the asphaltenes towards the top of the column (Elshahawi et al. 2007).

The asphaltene model in Chapter III describes the interaction between the properties of oil and their influence on the solubility and gravity term. GOR and density are of main interest in this context.

There is a desire to understand how the methane charge from the top of the column results in a change in GOR and density over time. A one-dimensional simulation model is designed to mimic these processes. The charge of methane in the oil column is represented by a portion of the grid-blocks at the top. This part of the grid is filled with 100% methane. The processes that take place in the gas-part of the model are of little interest to the study. The methane charge overlays a black oil column. The evaluation of oil density, GOR, and methane mole fraction as a function of depth in the oil column are the primary interest. The rate of change of these properties is directly linked to the destabilization of the asphaltenes.

The model consists of a vertical stack of grid-blocks (Figure V.3). A fraction of the grid-blocks at the top are filled with 100% methane to represent the secondary charge into the oil column. The bottom grid-blocks are filled with black oil. The model consists of a 30 cell large methane charge into a 120 cell high oil column. One cell is 1000mx1000mx5m large, resulting in a 600m tall oil column.

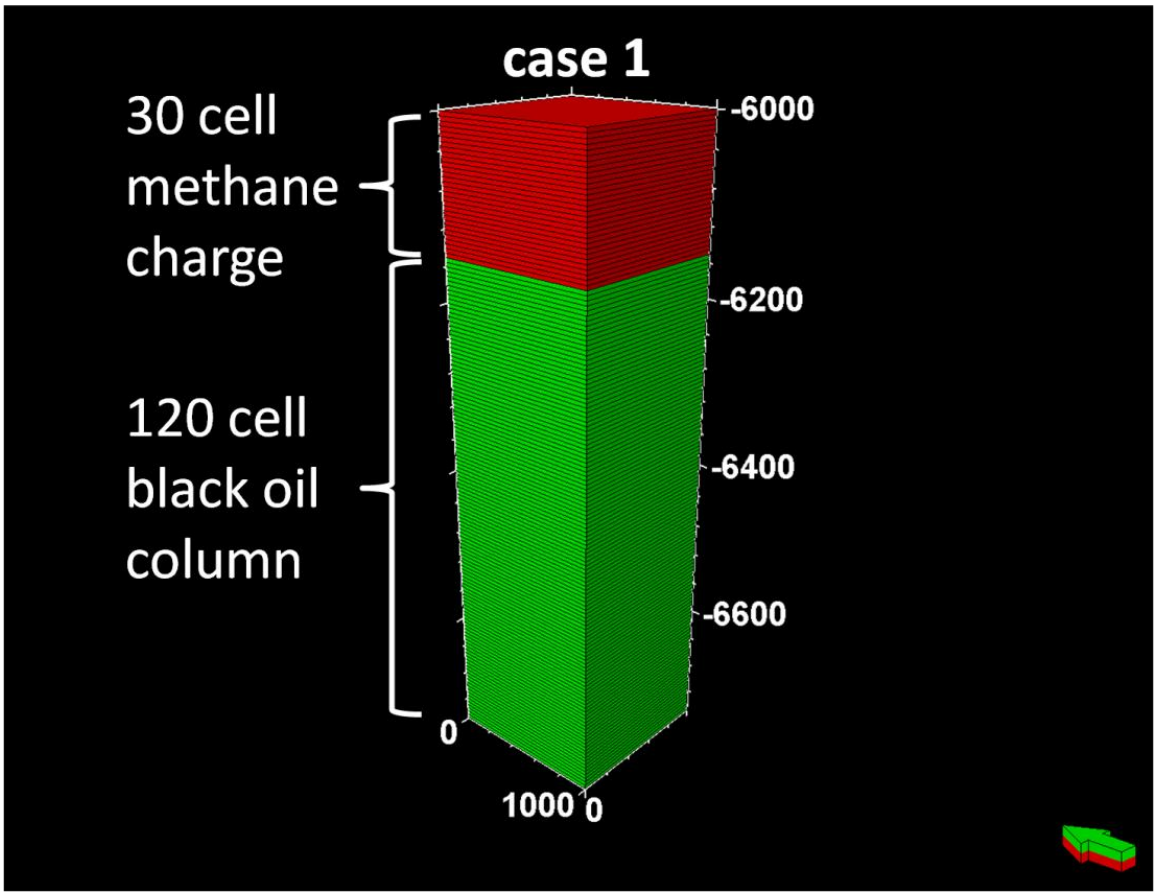

Figure V.3 – Simple one dimensional reservoir model to assess the evaluation of oil density, GOR, and methane mole fraction over geological time scales. The model consists of a 30 cell large methane charge into a 120 cell high oil column. The dimensions of one cell are 1000mx1000mx5m.

The following properties are used: the porosity in the grid is assumed to be 20%. The horizontal permeability is 1000mD and the vertical permeability is 100mD. Relative permeability curves are symmetric straight lines; the capillary pressure is assumed to be zero.

Prior to the late methane charge the reservoir is assumed to be filled with a low-GOR black oil. The pseudo components are modeled after a real black oil lab report. Obviously the laboratory report has to come from a different reservoir than the one of

the case study. Ideally the outcome of the simulation would show fluid property gradients that mimic the present day fluid in the reservoir. Splitting and grouping of the components was done as described in Chapter IV. Reservoir temperature and pressure are set to the values found in the example laboratory report of a black oil with a GOR of less than 300 scf/STB. The composition of the oil is grouped into eight pseudo components as depicted in Figure V.4. Diffusion coefficients are calculated as described in Chapter IV. They are tabulated in Table V.1.

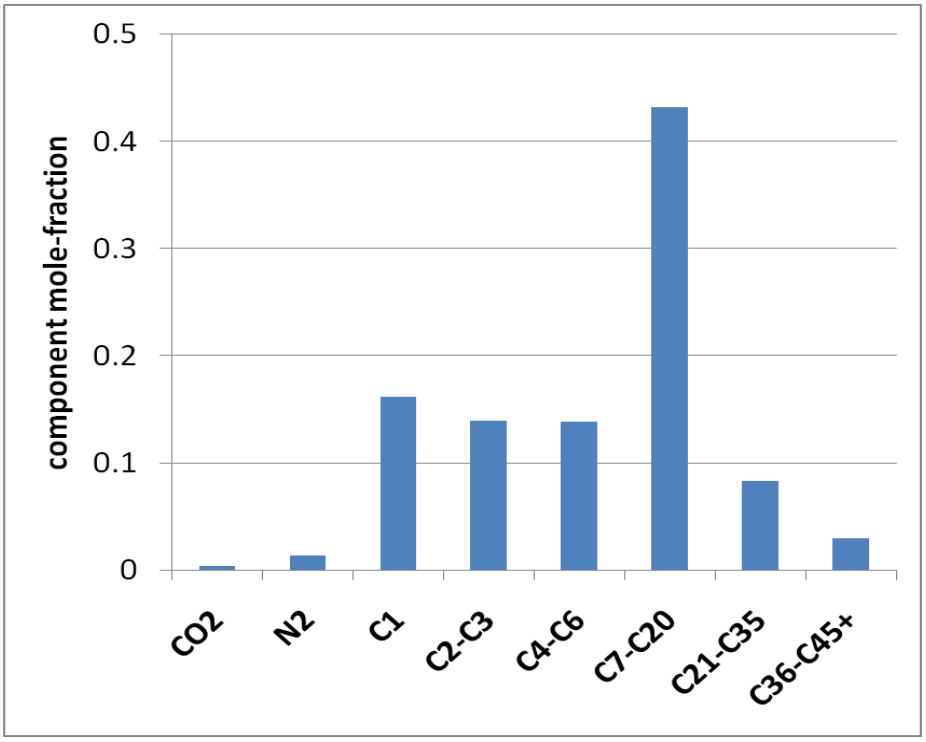

Figure V.4 – Initial fluid composition. Low GOR black oil grouped into 8 pseudo components.

Table V.1 – Diffusion coefficients of the pseudo components. In ECLIPSE*: DIFFAGAS denotes the activity corrected diffusion coefficient of the component in gas phase. DIFFAOIL denotes the activity corrected diffusion coefficient of the component in liquid phase

	DIFFAGAS	DIFFAOIL
pseudo component	[m^2/day]	[m^2/day]
C1	3.9813E-03	8.8544E-04
N2	3.9813E-03	8.8544E-04
C2-C3	2.5606E-03	5.6948E-04
CO2	2.5606E-03	5.6948E-04
C4-C6	2.0139E-03	4.4789E-04
C7-C20	1.0232E-03	2.2756E-04
C21-C35	6.5709E-04	1.4614E-04
C36-C45+	4.7503E-04	1.0565E-04

Figure V.5 shows the property curves at various times. At 10 million years and 16 million years the curves overlay. This indicates that equilibration in this column has been reached by 10 million years. At the top of the oil column, at the entry point of the methane, the fluid properties change the most over time. The rate of change in properties is reduced deeper in the column.

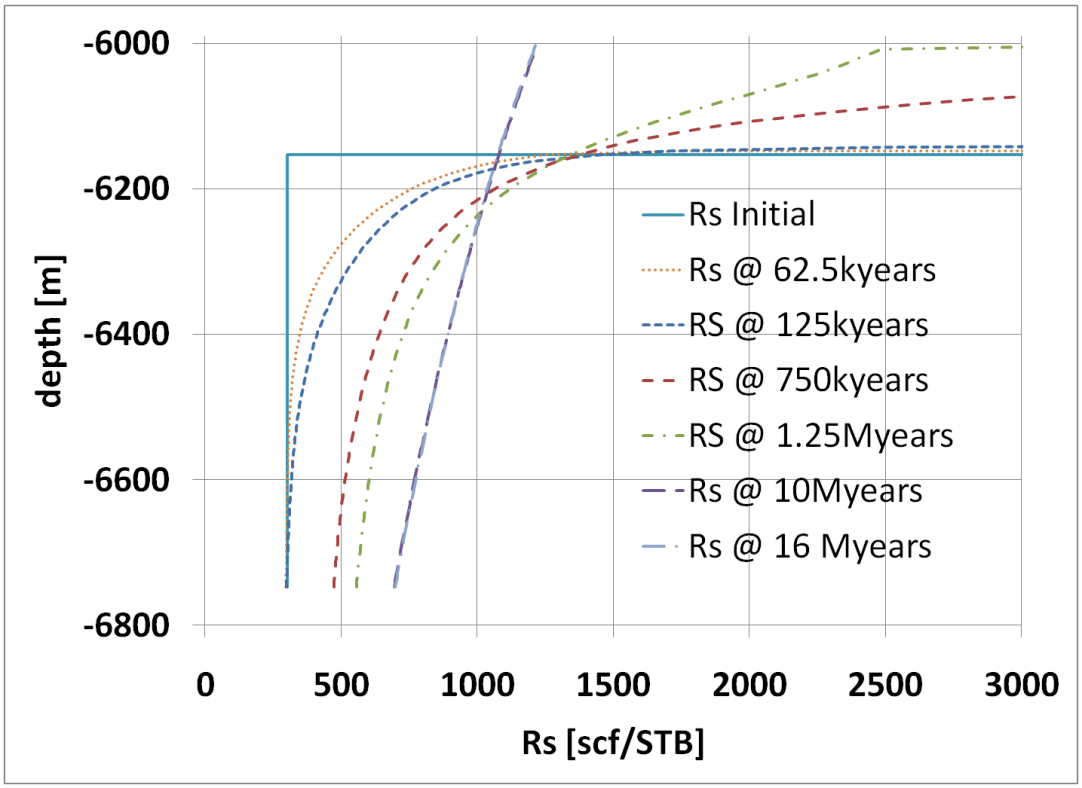

Figure V.5 – Solution gas against depth for various time steps. As the column equilibrates the magnitude of the gradient reduces.

The methane mole fraction of the mixture is closely linked to the GOR and the oil mass density. As expected these properties follow each other in terms of shape and distribution (Figures V.6 and V.7)

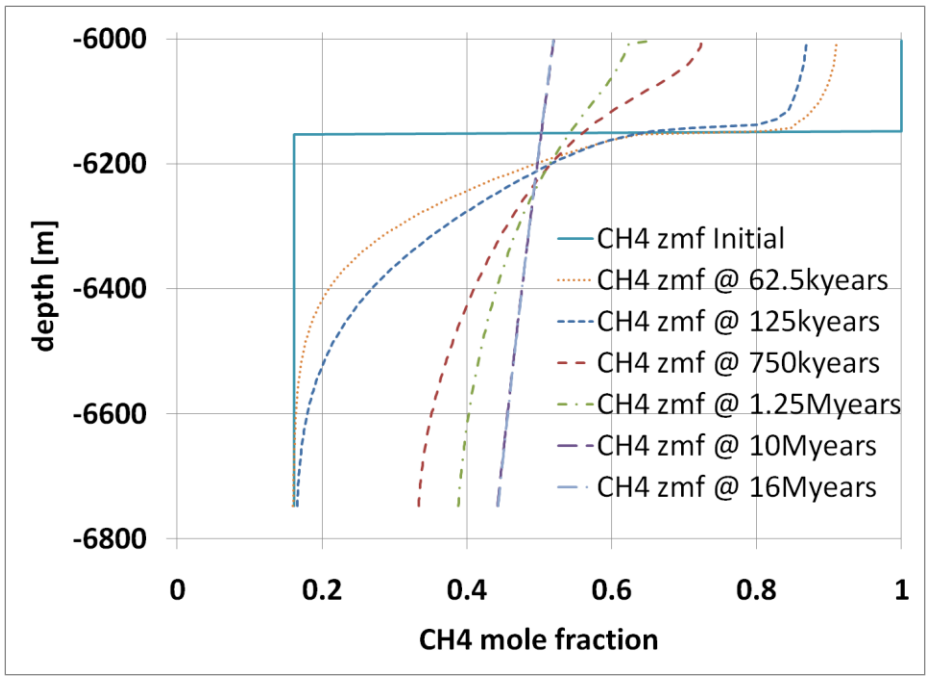

Figure V.6 – Methane mole fraction against depth for various time steps.

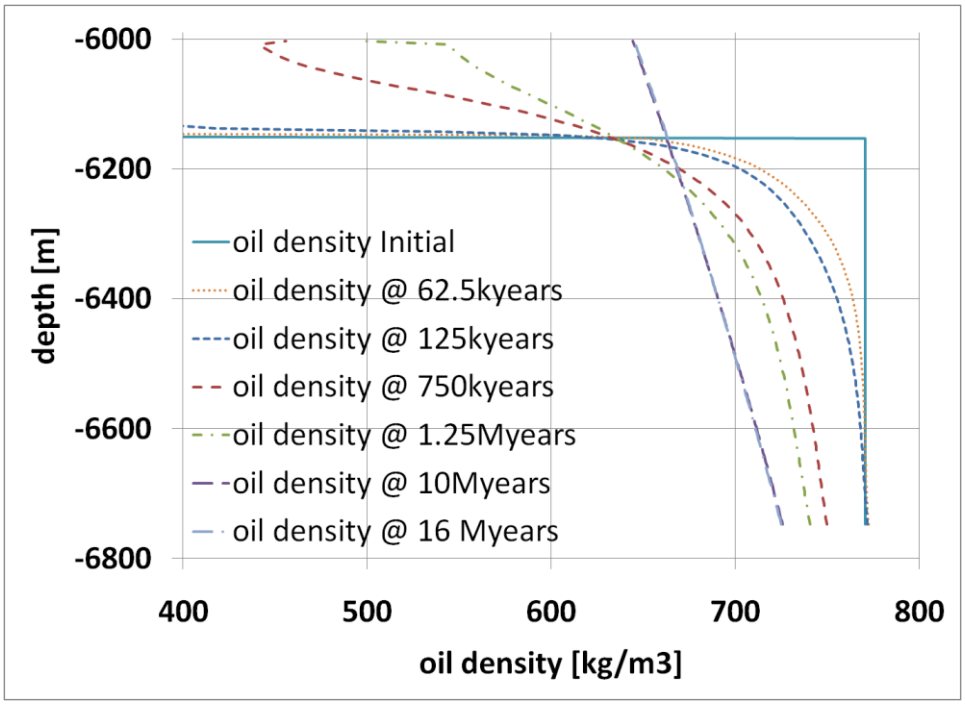

Figure V.7 – Crude oil density against depth for various time steps.

Higher oil density reduces the density contrast to the asphaltenes thus giving the particles less negative buoyancy. A higher GOR affects the solubility of asphaltenes at the same time. The density gradient here is only based on the change in composition of the oil column with regards to depth and time. The current simulation model shows how changes in oil properties can drive the mechanisms that impact asphaltene gradients. The recently developed asphaltene model is not yet incorporated into commercial reservoir simulators such as ECLIPSE*. Thus the combined effect of the oil and asphaltenes on GOR and density is not shown here. It can be expected to increase the magnitude of the gradients.

Case 2: Exceptionally Large CO2 Gradient in the Presence of Multiple Faults

A DFA campaign was run in a field in the Malay Basin with the objective to evaluate the connectivity between fault blocks. The field is situated in shallow water depth in an anticline structure of channeled sandstones and shallow marine sands. The reservoir is interbeded with mudstones of transgressive shale and marine shale (Harfoushian et al. 2008; Multalib et al. 2010). The map shown in Figure V.8 reveals the anticline structure of the field, shows the position of the wells, and shades what is believed to be different fault-blocks in different colors.

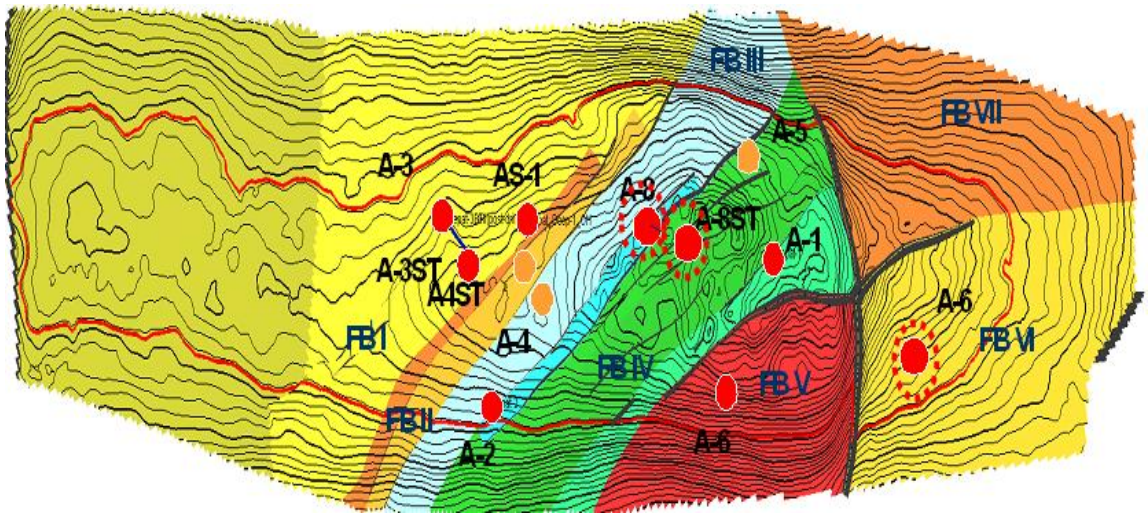

Figure V.8 – Well placement and fault blocks of a field in the Malay Basin, Malaysia (Harfoushian et al. 2008).

The DFA data was compared to previously taken MDT samples and samples from drill stem tests. The results show good agreement between the DFA and the lab data. This case is of specific interest since carbon dioxide is found in high concentrations in the gas cap of the reservoir and in lesser concentration in the oil column. The oil has a low GOR in the range from 477 scf/STB to 243 scf/STB. Part of the paper by Harfoushian et al. is concerned with the acquisition of representative CO2 samples in the presence of water. Focused sampling using the quicksilver probe, combined with the latest technology in DFA tools was key to the data acquisition (Harfoushian et al. 2008; Multalib et al. 2010). A large gradient in CO2, shown in Figure V.9, is revealed by DFA and confirmed by laboratory work. A relatively high concentration of CO2, above 60%mole, is found in the gas cap at different locations in the reservoir. The CO2 concentration in the oil column is monotonously declining down to concentration of only 2%mole at the bottom. GOR data and pressure gradients are also shown. There is a

smaller concentration measured in Well A-8 at shallower depth than in Well A-7 at deeper depth. Well A-7 is not labeled on the map. The well is suspected to be on the east side of the gas cap, whereas Well A-8 is on the west side of the map. Note that there are two wells labeled as A6 in the east of the field and Well A-7 is missing. Well A-7 can be considered as an outlier. The gradient in the western direction of the gas cap is monotonous with a falling CO2 concentration with depth. It stretches across two faults.

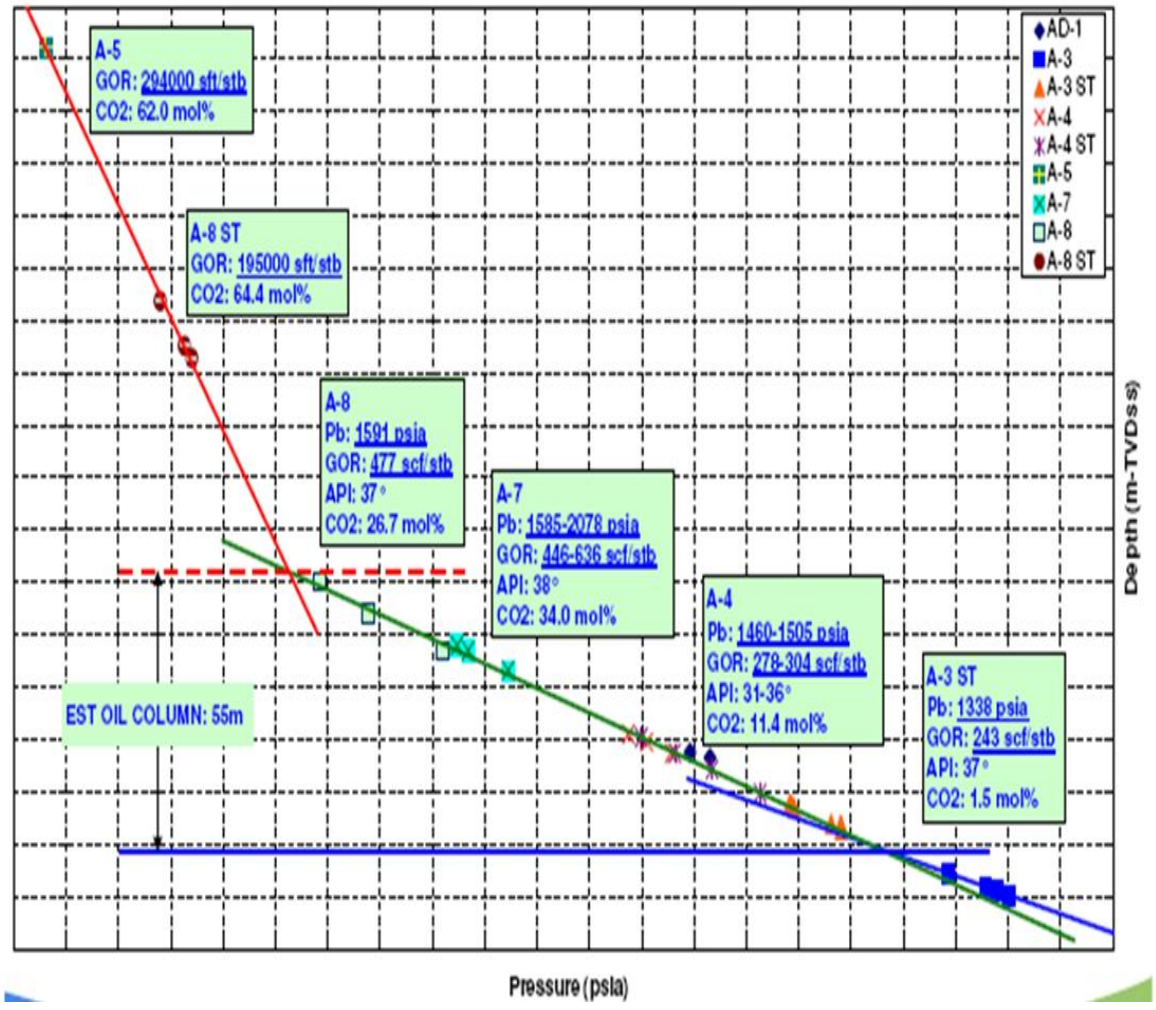

Figure V.9 – GOR and CO2 concentration vs depth in a field in the Malay Basin (Multalib et al. 2010).

A plausible explanation for this gradient would be a diffusion process that charges CO2 from the gas cap into the oil column. Using this monotonous CO2 gradient as a benchmark, a one-dimensional diffusion model shall back this hypothesis.

A number of variables can be adjusted to make a match between the real gradient and the simulated gradient. Most of those variables are unknown. Therefore the best the model can do under those conditions is a zeroth-order approximation. A strategy can be derived from this approximation to study higher order effects and essentially improve the understanding of the real reservoir architecture.

The model's dimensions are an educated guess on the lateral diffusion length. The height of the oil column is known to be 55m TVD. This marks the lower boundary in terms of length. Lateral distances between the wells can increase the diffusion length largely. Under this consideration, a column height of 500m is not unreasonable. The model will be tilted 45 degrees to introduce gravity effects and reflect the angle of the geologic structure. Porosity and permeability will be left uniform throughout the model. If not mentioned differently the properties of the model are as in the model of Chapter IV. A series of sensitivities has been evaluated to see the effect of initial composition, diffusion length and the influence of barriers. Figure V.10 shows visualization the model.

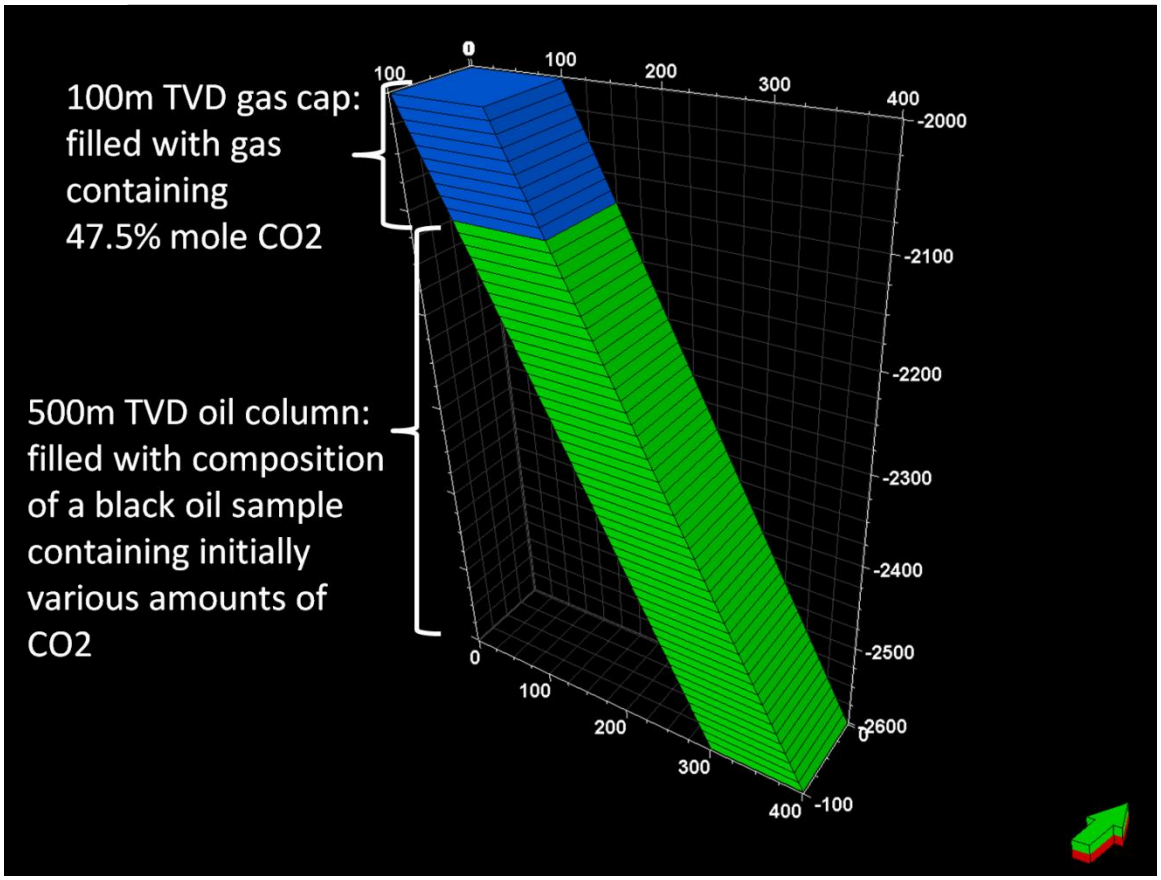

Figure V.10 – Titled vertical one-dimensional model to investigate CO2 charging into an oil column.

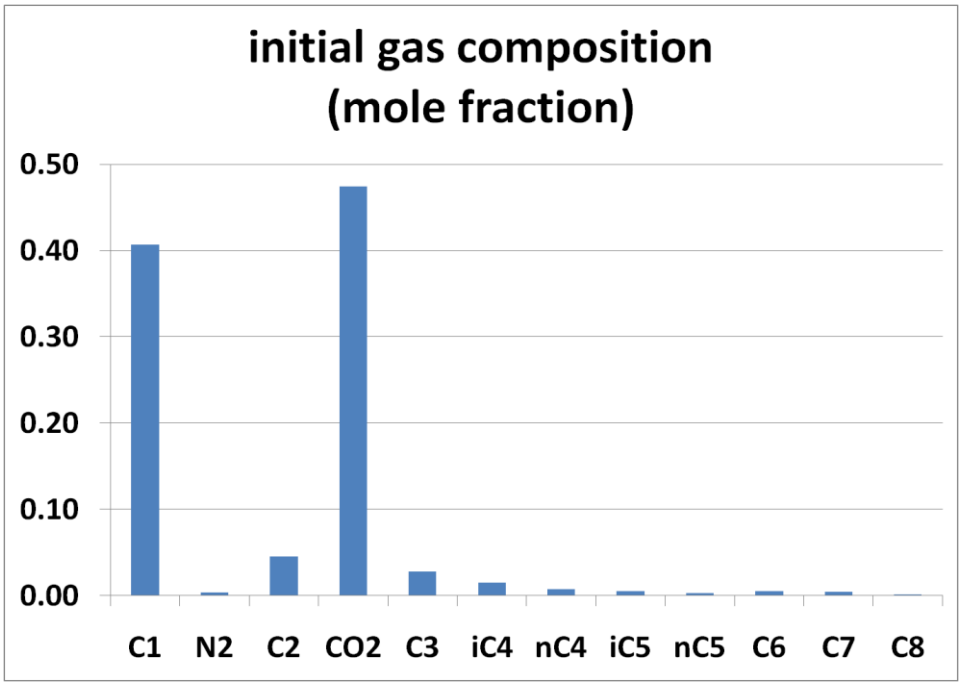

Figure V.11 – Initial gas composition with a CO2 content of almost 50% mole.

The initial composition of the gas and the oil is unknown. The gas cap is initialized with a gas of high CO2 content, similar to what has been seen in the Malay Basin field. The composition of the gas is shown in Figure V.11..

The initial content of CO2 in the oil column will determine the magnitude of the initial chemical gradient across the phase boundary. To investigate the influence of this initial condition, four cases vary the CO2 content in the oil. Figure V.12 shows the oil composition for each of the cases. To change the composition of the CO2 in the oil, all necessary calculations respect the weight fraction of the components, i.e. the sum of all weight fractions of all components is kept constant. The resulting new composition is then converted back to mole fractions.

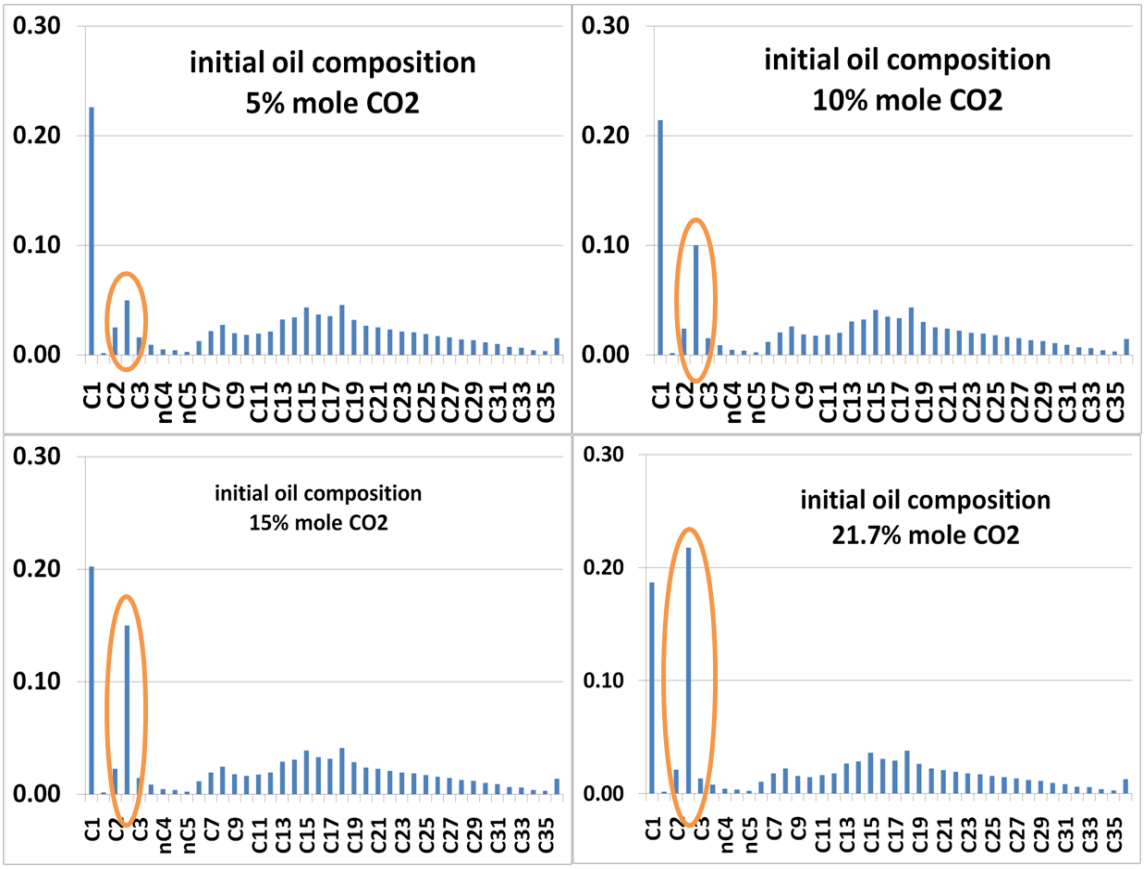

Figure V.12 – Initial oil composition - four different cases. The initial oil composition has been varied 21.7% mole to 5% mole.

After the model is initialized, diffusion and gravity will mix the components. The change of the CO2 composition with depth is plotted for various points in time and presented in Figure V.13. The largest gradients are seen within the first 200 thousand years. After that CO2 continues to diffuse from the gas cap into the oil column and continuously raises the CO2 concentration at the bottom of the oil column. The largest gradient is seen in the case that started out with the lowest concentration of CO2 in the oil. The gradients at 10 million years and 16 million years overlay, suggesting that a steady state has been reached at 10 million years.

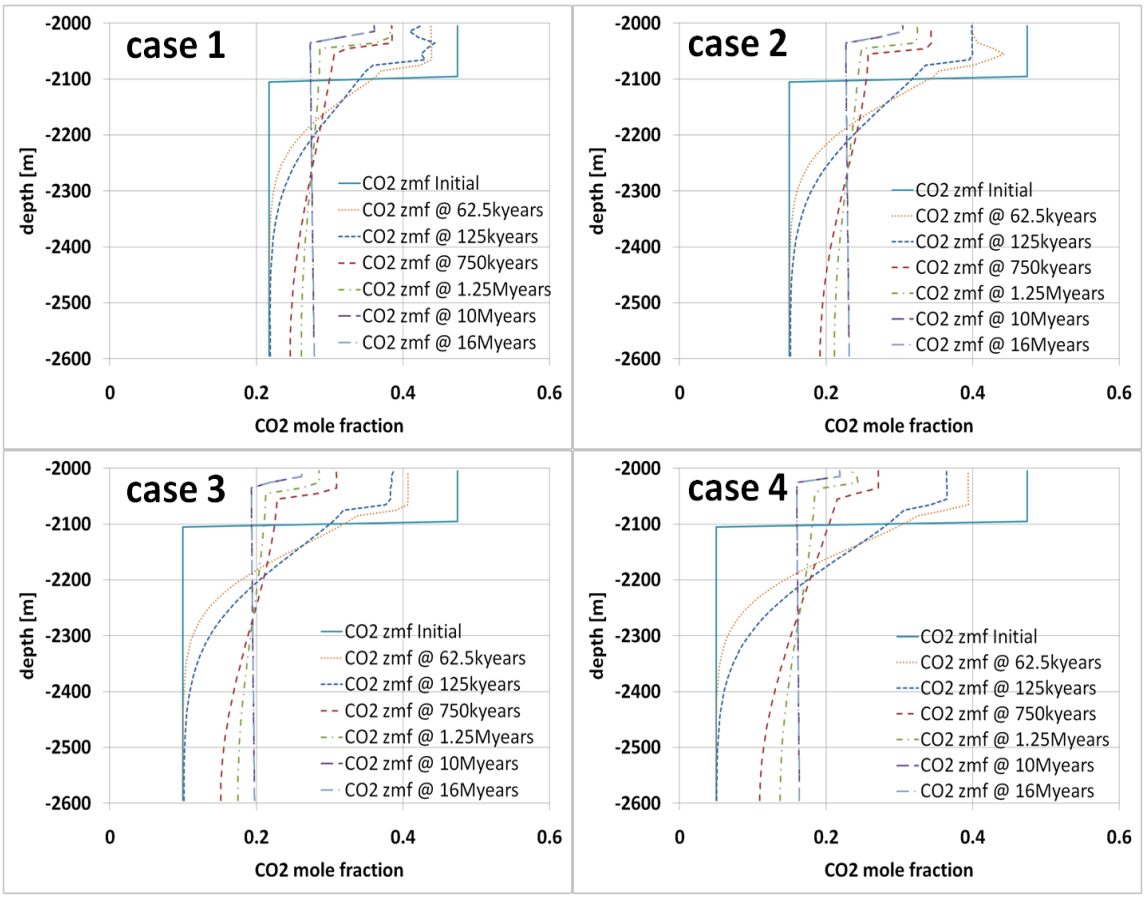

Figure V.13 – CO2 gradient evolution for different initial oil compositions.

Given the constant diffusion length for these cases, the time to equilibrate the system is constant for all cases. A further study shows the influence of the diffusion length on equilibration time. The model is initialized with a CO2 concentration in the oil of 5% mole. The height of the oil column is varied in four steps: 60m, 180m, 300m and 420m. To evaluate the equilibration time, the CO2 concentration is probed at three different depths for all cases: Just below the gas oil contact, in the middle and at the bottom of the oil column. The CO2 concentration at these depths is plotted against time in Figure V.14.

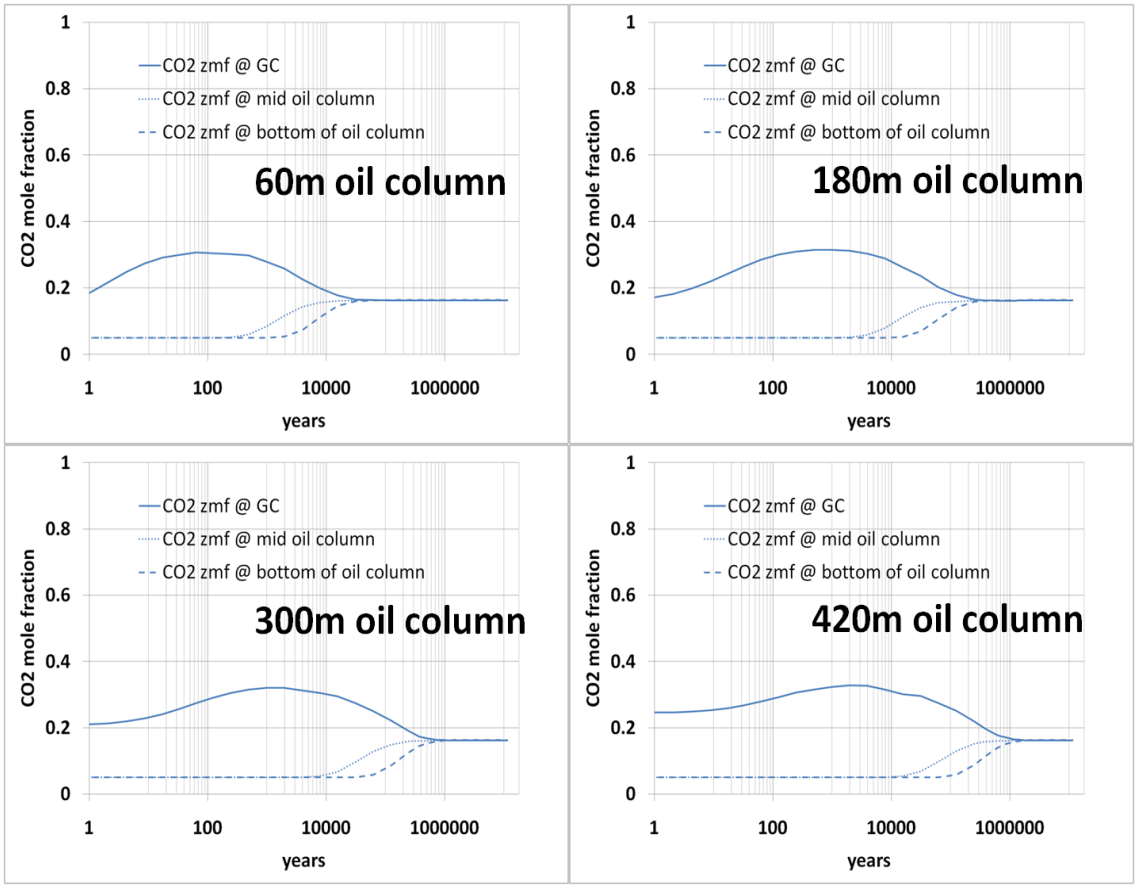

Figure V.14 – Different diffusion lengths and their influence on equilibration time.

The equilibration time may stretch to up to one million years for a distance of 420m. The concentration at the bottom of the column stays at the initially low CO2 concentration for at least two thirds of that time. This observation is in line with the low concentrations measured in the deepest parts of the reservoir.

The map of the field shows a number of faults and fault blocks. The flow communication across these faults is of high interest when planning the field development. The influence of the presence of a fault on the gradient is investigated in the one-dimensional model. The initial gas and oil composition is shown in Figure V.15.

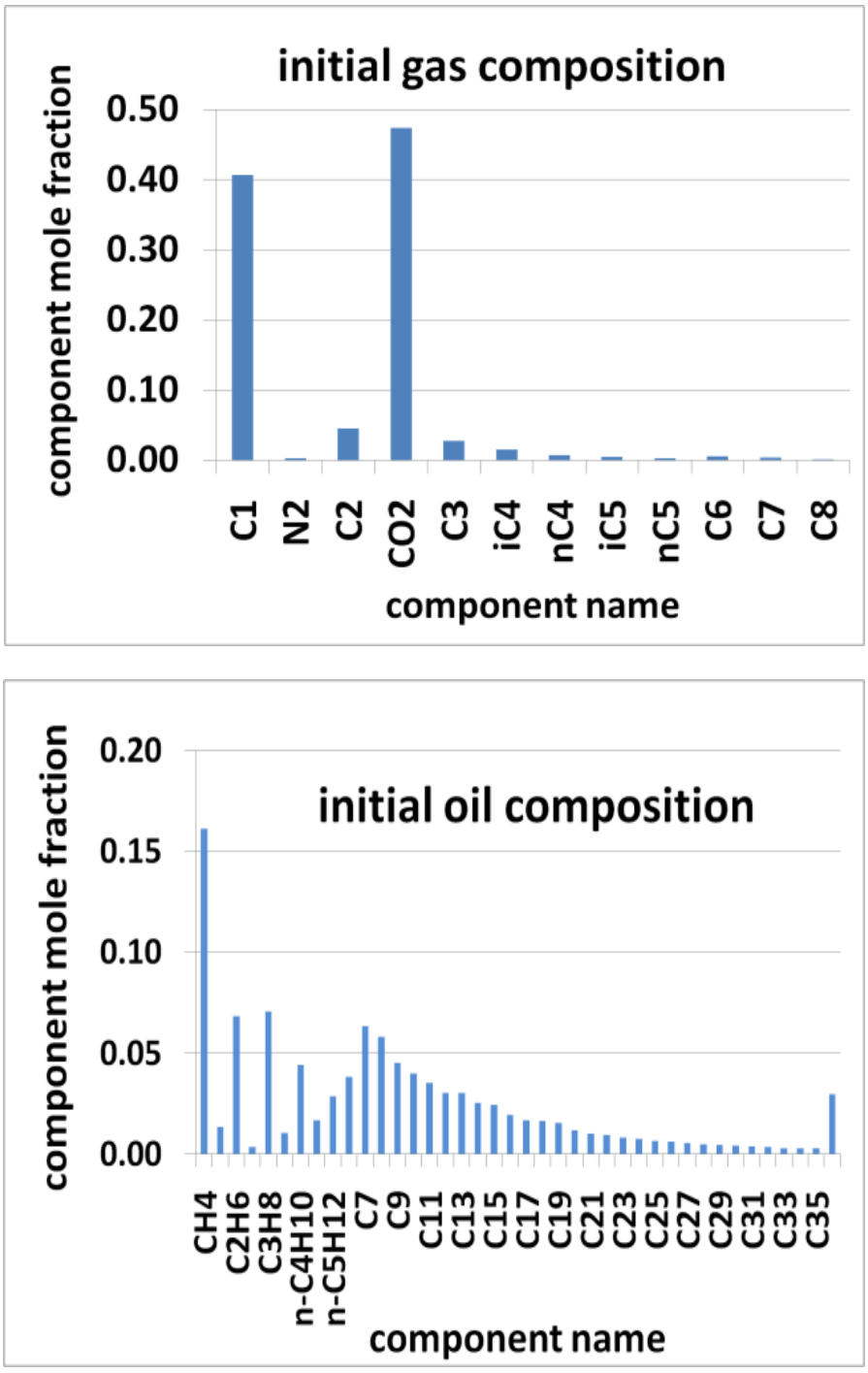

Figure V.15 – Initial composition of the gas contained in the gas cap (top) and the oil column (bottom).

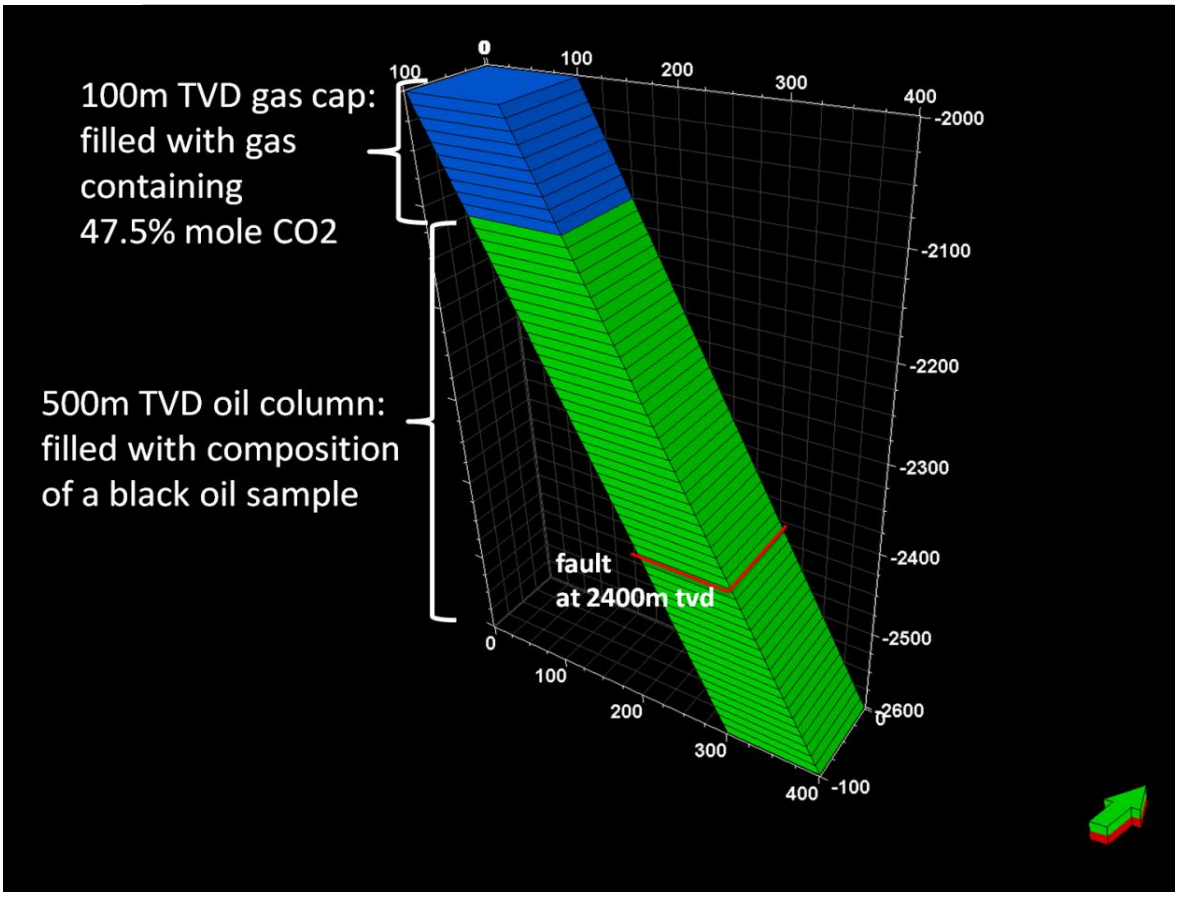

Figure V.16 – Tilted one-dimensional model with fault.

A fault is introduced to the model as shown in Figure V.16. The resulting CO2 concentration is plotted versus depth for various moments in time in Figure V.17. A fault introduces a step change in the fluid profile. The magnitude of the step depends on the transmissivity of the fault.

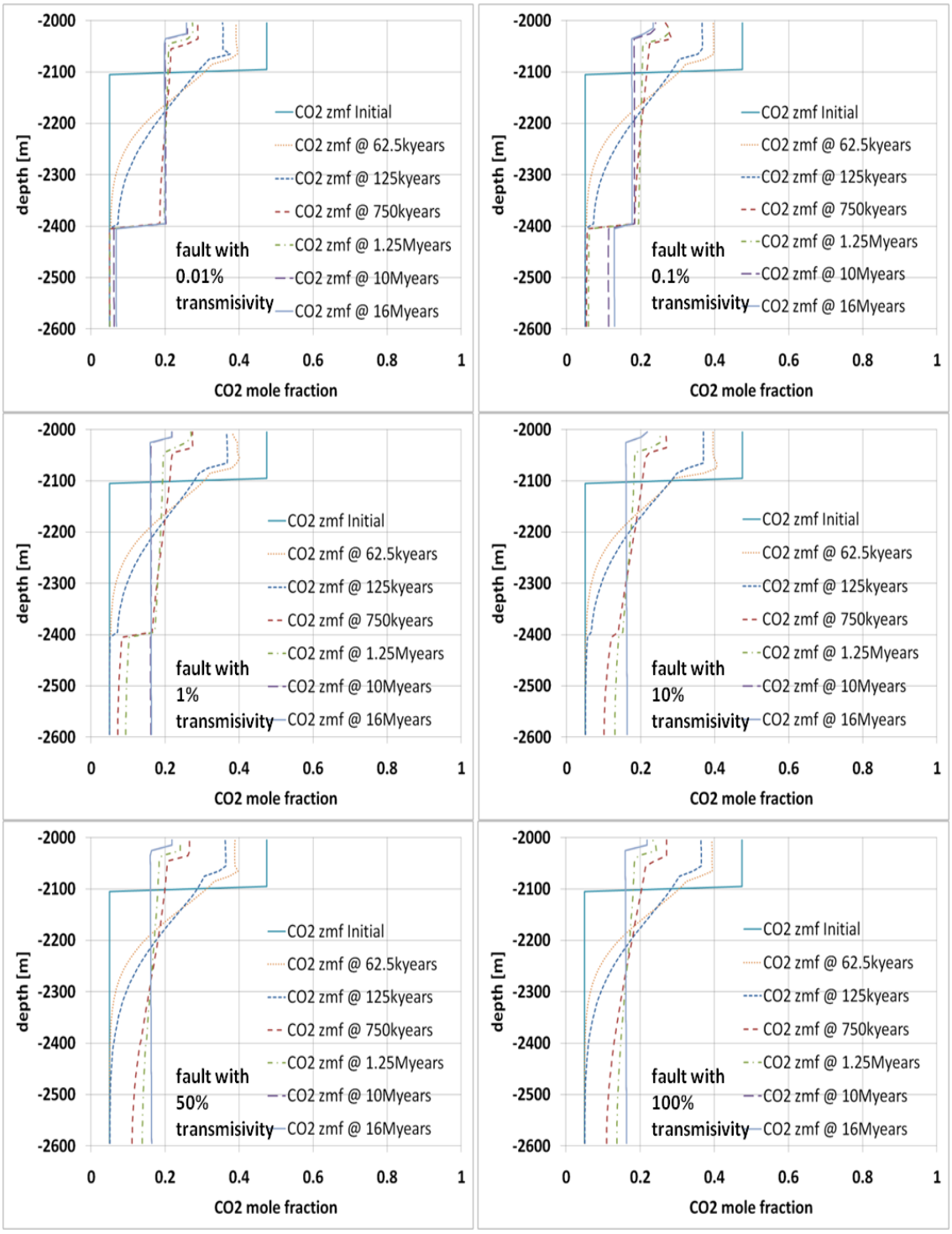

Figure V.17 – Influence of a fault on CO2 gradient. A fault at 2400m is common in all of the above fluid profiles. The transmissivity of the fault varies from 0.01% to 100%, resulting in a step change of CO2 concentration of different magnitude.

The simulation runs so far have given an idea of how the model reacts to different variables and initial conditions. A fault introduces a step change in the gradient. The question regarding whether the fault blocks in the field are in flow communication remains still open. The only data available for comparison are the data points shown in Figure V.9. According to this information the CO2 content in Well A-3ST, at the bottom of the oil column is 1.5%. Well A-4, in the middle of the oil column, has a CO2 concentration of 11.4%. Well A-8 shows a CO2 concentration of 27.6%, just below the GOC. On the map each of these wells is situated in a different fault block.

A base case simulation model assumes all faults are 100% transmissive, i.e. no barriers are present. It is set up with a high initial CO2 concentration in the gas cap and zero CO2 content in the oil column. The largest gradient after around 250,000 years lines up well with the data measured in the three wells (see Figure V.18).

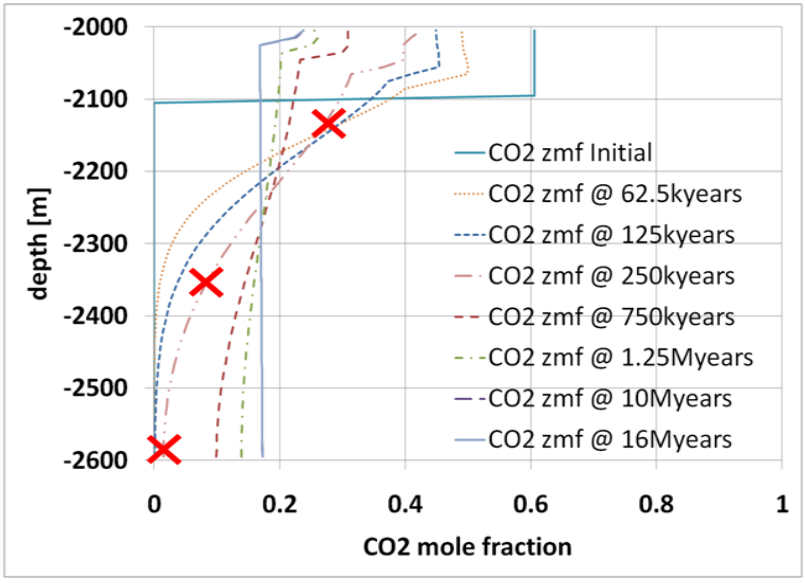

Figure V.18 – Base case simulation without barriers. The red crosses are the data points as measured in the field. A good match between simulation and data is found in the 250000 year gradient line.

The map (Figure V.8) suggests the presence of possibly sealing faults. Two faults are introduced in the model between the wells. At first the pressure profile is modeled to investigate the timescale of pressure equilibration. For two faults with a transmissivity of 0.01% the pressure equilibrates within 125 years. Figure V.19 shows the evolution of the pressure gradients with time. The initial pressure is uniform throughout the column.

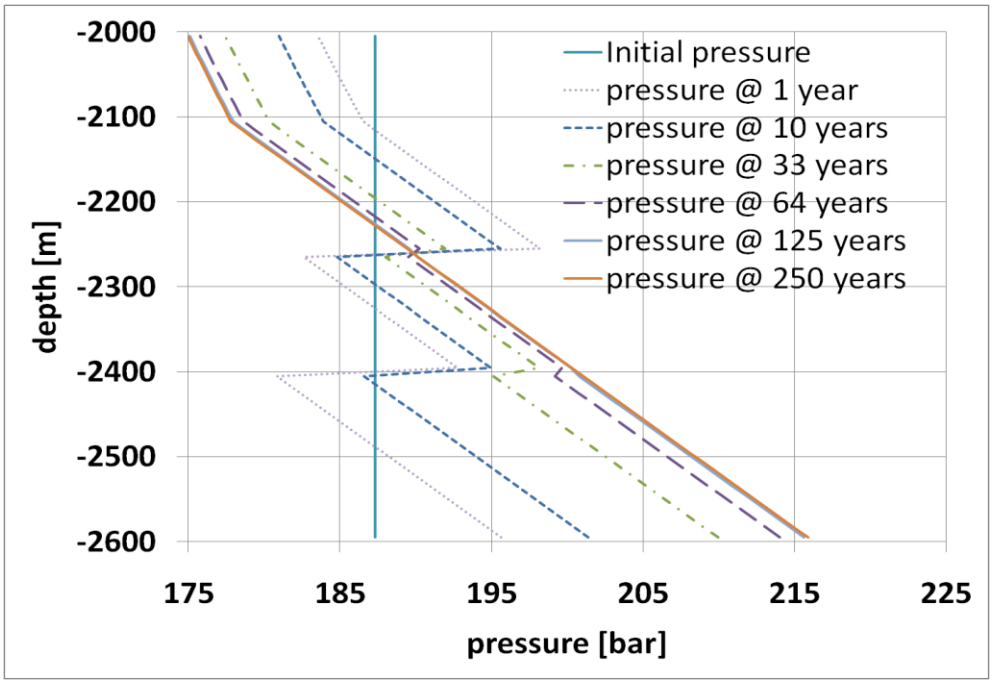

Figure V.19 – Evolution of the pressure gradient over time. Equilibration is reached after only 125 years. After that the pressure gradient fails to identify the flow barrier in form of two faults with a transmissivity of 0.01%.

The CO2 gradient in the presence of two faults was investigated next. Various simulations were run. The transmissivity of the faults was varied over a range from 100% to 0.01%. Two plots are presented here. In each plot one of the gradients lines up with the data points. This suggests that a match like in the case without faults can be

found in the presence of faults. Figure V.20 shows the resulting gradients for a fault transmissivity of 1%. Figure V.21 presents the gradients that result from faults of 0.01% transmissivity.

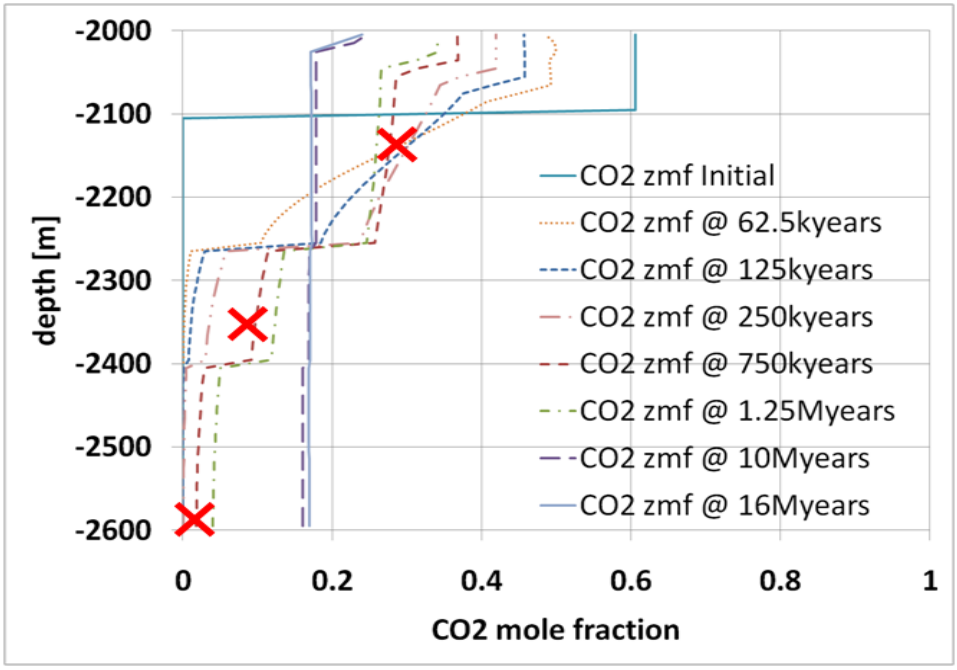

Figure V.20 – Results of the simulation model with two faults of 1% transmissivity. The gradient at 750,000 years matches the data measured in the field.

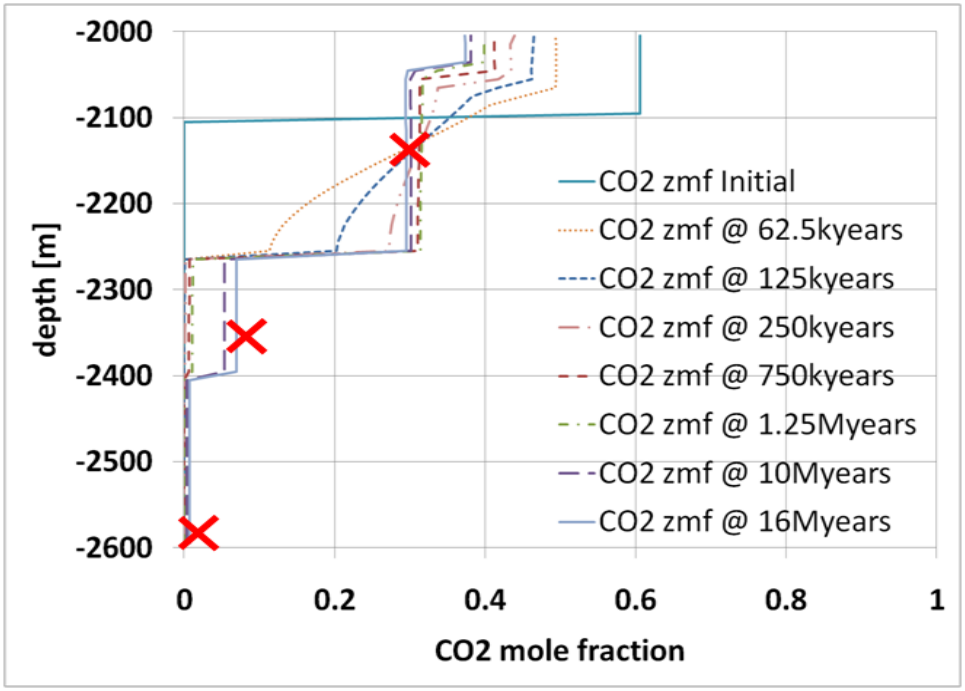

Figure V.21 – Results of the simulation model with two faults of 0.01% transmissivity. The data suggests that a gradient after 16million yeas matches the data measured in the field. Please notice the vertical profile between the faults. A feature that is missed by having only one data point per fault block.

In the absence of faults and in the faulted case the data points may be lined up with a gradient. In the absence of hard data, all of the following reasoning is purely speculative. Yet under reasonable assumptions one scenario is more likely, to occur than the other.

It needs to be noted that CO2 in such high concentration is not liberated from kerogen. Thus the hydrocarbon and the CO2 charge the reservoir come from two different locations. Both simulation cases (faulted and unfaulted) introduce the CO2 from the top. Charging the CO2 exclusively from the top makes sense for the unfaulted case. If the entire reservoir is connected the light CO2 may enter the reservoir on a high

mobility charge plane. It accumulates at the top without percolating uniformly through the oil column. This scenario would be in line with Stainforth's charge model (Stainforth 2004). After its accumulation at the top, CO2 diffuses into the oil column. As a result, a large continuous and monotonous gradient is formed.

The case of sealing faults seems contrived to match the data and raises a number of questions: How does the CO2 reach the gas cap without getting trapped lower in the column? The reservoir would have needed to be charged with hydrocarbon fluid. If it was faulted subsequently it would be likely that it would lose its charge in the process. Subsequently the CO2 would have needed to find a way into the gas cap without getting trapped at the faults lower in the column. Compared connectivity-scenario the case of sealing faults is less likely to occur.

Another uncertainty is the age of the reservoir and the time line of the petroleum system. Which fluid gradient needs to be assessed? The match in the case of no flow barriers is found on a transient gradient at 250,000 years. The match in the case of the two faults with a transmissivity of 1% is found at 750,000 years and in the case of two faults with 0.01% transmissivity the data suggests a match past 16 million years.

There is only one data point in each fault block available and therefore it is hard to make an assumption of the shape of the gradient within the fault block. Knowledge of the shape of the gradient within the fault block would largely increase the confidence of the interpretation. It would help to identify the gradient that applies and make it easier to conclude a firm statement about compartmentalization. Additional DFA data points within each fault block would yield that knowledge.

With the limited data available, no clear cut conclusion can be made on the connectivity of the fault blocks. A petroleum system model will need to explain how the CO2 and the hydrocarbon charges into the reservoir. This knowledge would certainly facilitate a decision on which case to consider.

The CO2 concentration exhibits the largest gradient in the data. Hence CO2 is the analyte of interest when trying to use gradients to constrain compartments. The GOR of black oil is less graded and thus not as suitable as an indicator to constrain compartments in this case. It is suggested to investigate the asphaltene gradient in this field since the difference in CO2 concentration might have impacted the stability of the asphaltene suspension.

Case 3: 2D Simulation of a Leaky Seal

An unpublished case of a leaky seal field is currently under investigation by DFA experts. In a field in Ghana, petrophysical well log data indicates that the gas cap is separated from the oil column by a 10m thick layer of shale. DFA data suggests that all components are in equilibrium across this barrier. This suggests that the gas and the oil are in flow communication. The geologist on the team mentioned that the shale layer may pinch out further away from the well. This would allow the gas cap to be in direct contact with the oil column (Mullins, 2010b).

To gain insight of how a fluid column would reach equilibrium in the presence of a discontinuous barrier or a leaky seal, a tow-dimensional model is designed. A lateral dimension in addition to a linear diffusion distance is needed to capture how gradients

form in such a case. The model is very similar to the one-dimensional models used earlier. Figure V.22 and V.23 summarize the properties of the model.

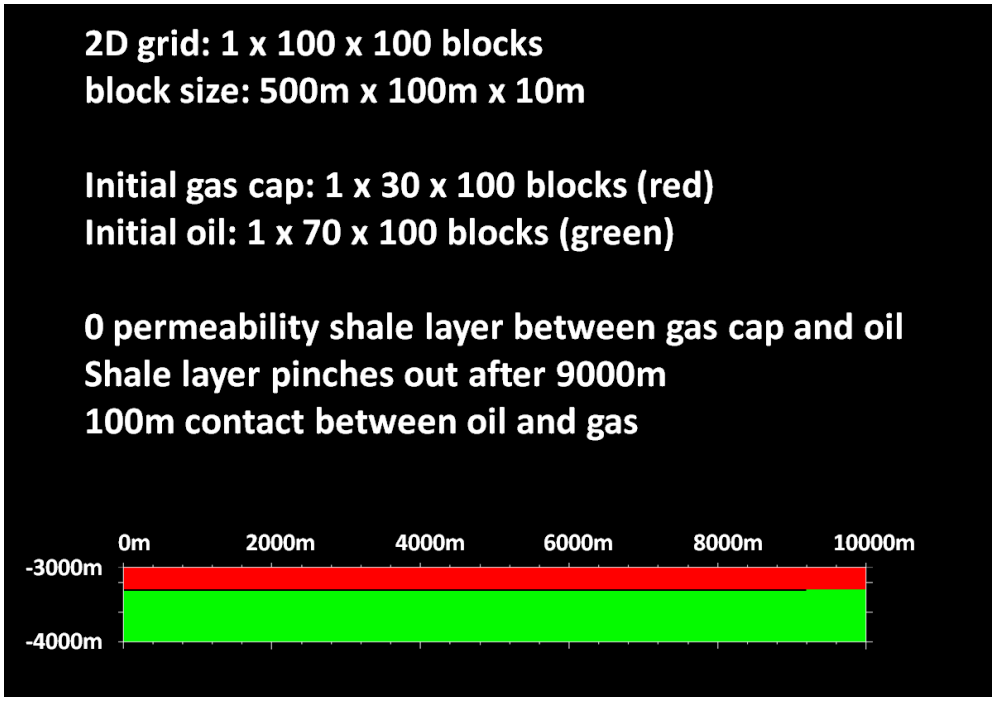

Figure V.22 – Grid properties of 2D model. The shale layer reaches almost all the way across, leaving only 100m of contact between gas and oil on the right side of the model.

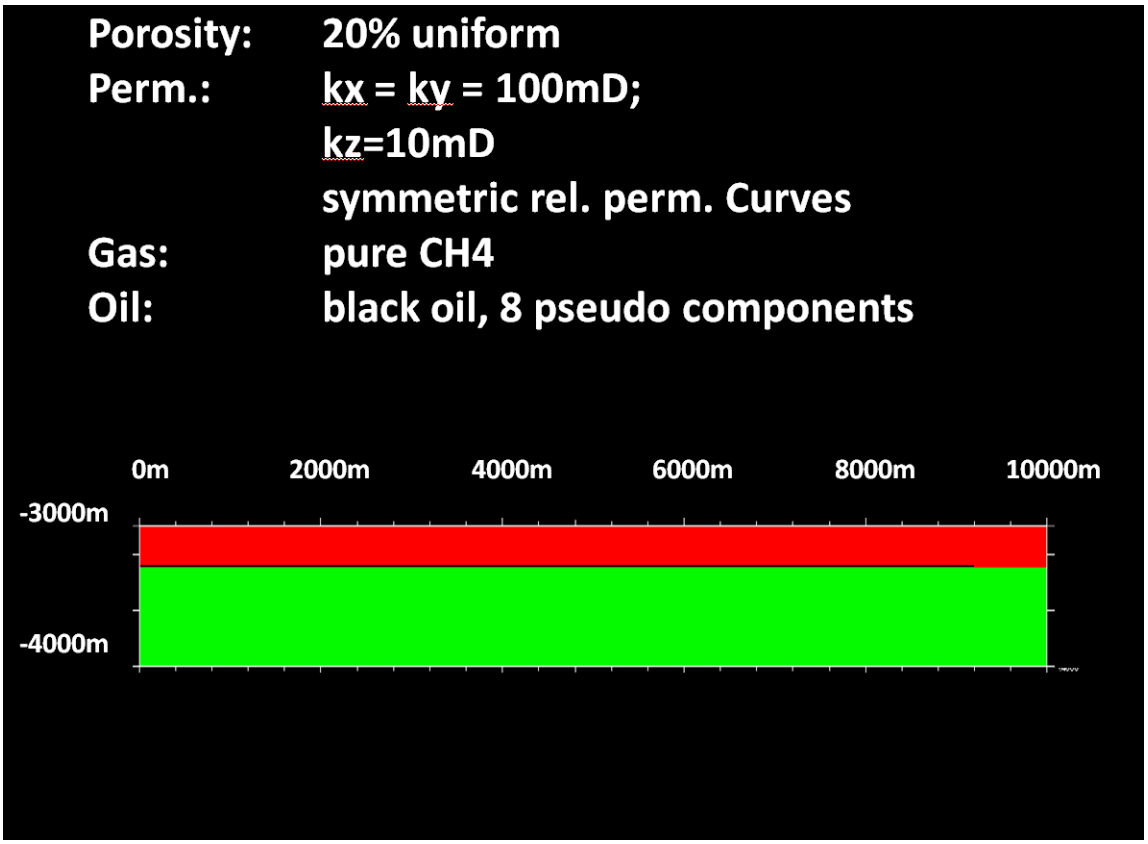

Figure V.23 – Rock properties and initial fluid properties of 2D model.

A series of simulation runs is planned for this model. One of the parameters that are of interest here is the influence of the contact area between to oil and the gas. In the first simulation run 90% of the contact area between gas and oil is covered by a row of gridblocks with zero porosity and zero permeability. Figure V.24 shows the evolution of the methane mole fraction with time. The column slowly equilibrates laterally.

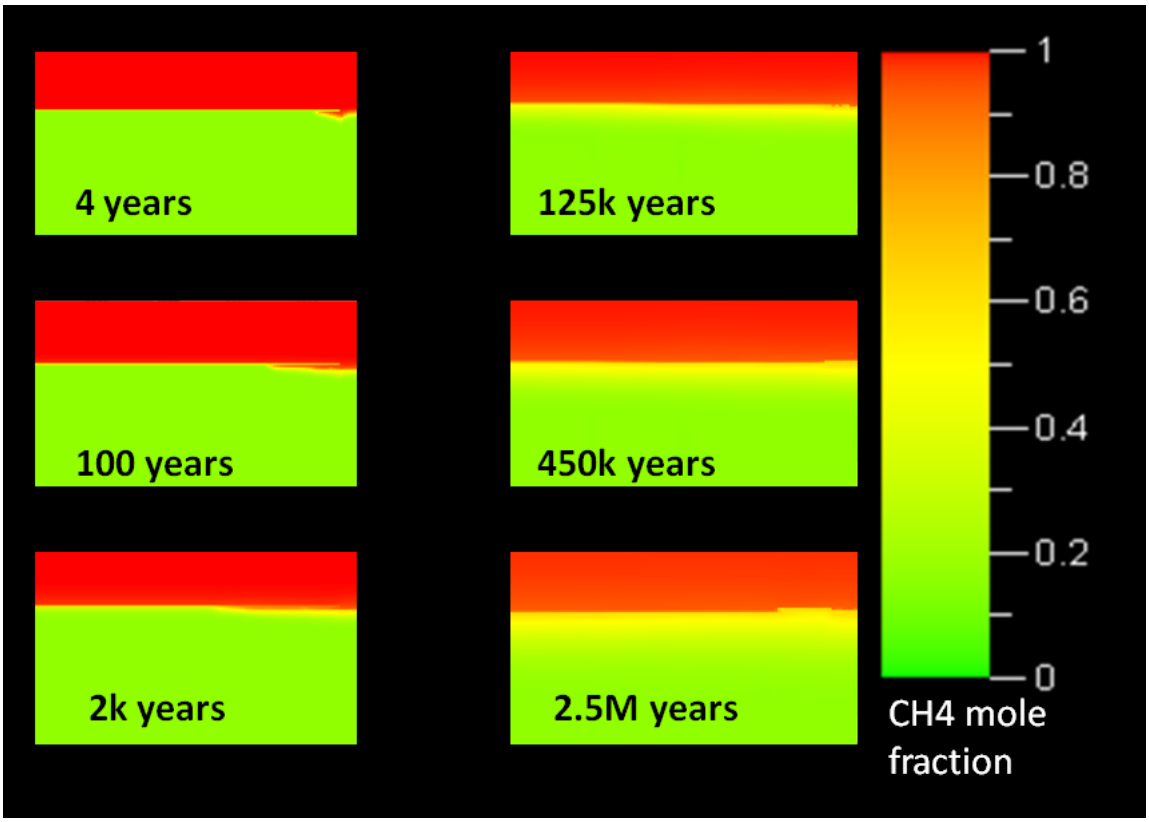

Figure V.24 – Evolution of methane mole fraction over time.

It was found that the simulations take a significantly large amount of time and computational power. In some cases it takes up to 3 days only to reach the next time step. It was observed that the vapor-liquid equilibrium calculations are responsible for these long computational times. The number of gridblocks was reduced from 100x100x1 to 50x50x1. The amount of gridblocks was found to have little to no effect on the runtime. In another approach the convergence criteria for the vapor-liquid calculations where loosened. This improved the run time to an acceptable level, yet the model did not equilibrate properly, leaving a residual lateral gradient. The results shown above were generated by a computer outside Texas A&M that allows four-way parallel processing.

While run times are still an issue with these simulations the results can be very interesting. A GOR profile is shown in Figure V.25. In this case the shale layer extends only half way across the model width. The color coding reflects the GOR distribution. Please note that Petrel computes a GOR of zero in the absence of a liquid phase. That is why the gas cap displays a GOR of zero. A value of infinity would be more appropriate. An interesting observation is the way gravity acts to pull heavier components towards the bottom of the column. This happens in a laterally non-uniform manner. As a result the GOR drops to low values between 40 and 60scf/STB. It is expected that after sufficient time these non uniformities will disappear and lateral equilibrium will be reached.

2D modeling requires significant amounts of time and computational power. Even though some progress was made, further investigation is needed to reduce the run time of the simulation.

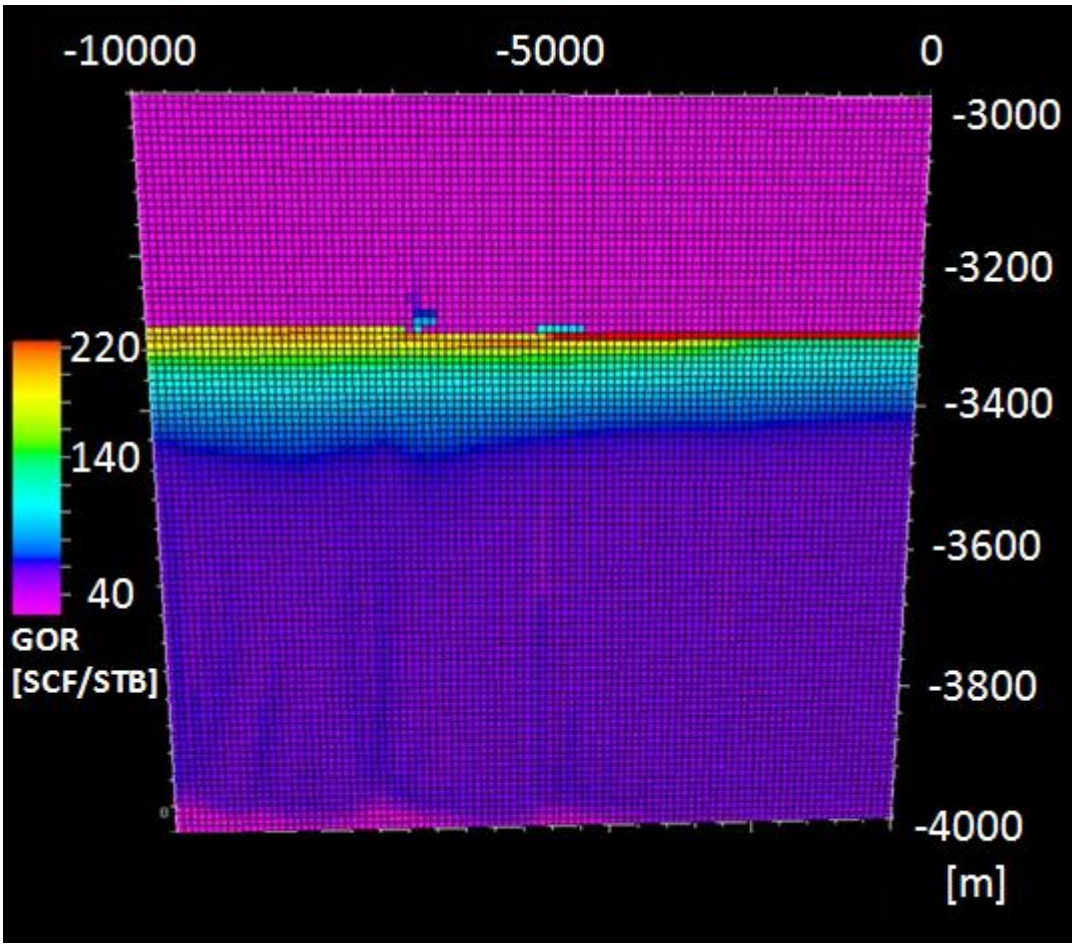

Figure V.25 – GOR distribution after 320 thousand years. Shale layer covers 50% of the contact area between gas and oil. Please note that gravitational effects accumulate heavier components at the bottom of the reservoir in a non-uniform manner. It is expected that after sufficient times lateral equilibration will be reached.

The field case has just recently come up and is not published yet. The result shown here so far is only an outlook on future modeling work. As more details on the field case become available, more focused work can be performed. Future sensitivities would include variations of the properties of the shale layer. At the moment zero porosity and permeability is assumed for the shale. Investigation of small amounts of diffusion flux across the shale is believed to be possible for light components depending

on the shale properties. This could be modeled and investigated in future simulations. Furthermore a study of the effect of initial composition is considered to be relevant.

In this chapter the use of simple simulation models in real field studies of fluid complexities was presented. The findings proved to be useful in explaining the origin of non-equilibrium fluid distributions and the possibility of their evolution towards equilibrium over time.

In Chapter VI recommendations about data acquisition in the presence of non-equilibrium fluid gradients, especially in the presence of faults will be discussed.

CHAPTER VI

RECOMMENDATIONS FOR DATA ACQUISITION AND CONCLUSIONS

DFA technology and its application has been summarized and put in the context of understanding reservoir architecture. The available interpretation techniques to model equilibrium fluid distributions have been summarized earlier in this work. Non-equilibrium columns pose a challenge, as they generally can not be modeled by a set of equations. A method of simple reservoir simulation has been introduced to investigate the diffusive flux in non-equilibrium fluid columns. Applications of these simple models have shown to be of help in interpreting the origin of large gradients. These simulations, in their simplicity will never be able to compete with a complex basin model in terms of accuracy. The intention is to make a prediction of the zeroth order physics. This prediction helps to define and focus the investigation of higher order effects.

Recommendations for Data Acquisition

A question that frequently arises is: How many DFA stations are needed to do these interpretations and predictions? Recommendations have been issued on how many DFA stations are needed in an equilibrium case. As discussed in Chapter III, there is a minimum of two stations needed to establish the EoS model. Further stations are then used to either refine the model or to reveal measurements of non-equilibrium fluids. Based on the observations in Chapter V, two further recommendations may be issued in case such non-equilibrium is revealed on a DFA station. The case study of the reservoir

in the Malay Basin serves as an example to illustrate the value of additional stations. It also shows that all available data needs to be used to maximize its value.

The publication of the Malay Basin CO2 case actually uses GOR plots to compare fluid composition on either side of the fault blocks. Figure VI.1 schematically shows the location of wells with respect to suggested faults (Multalib et al. 2010). Figure VI.2 shows compositional plots based on the data acquired in these wells.

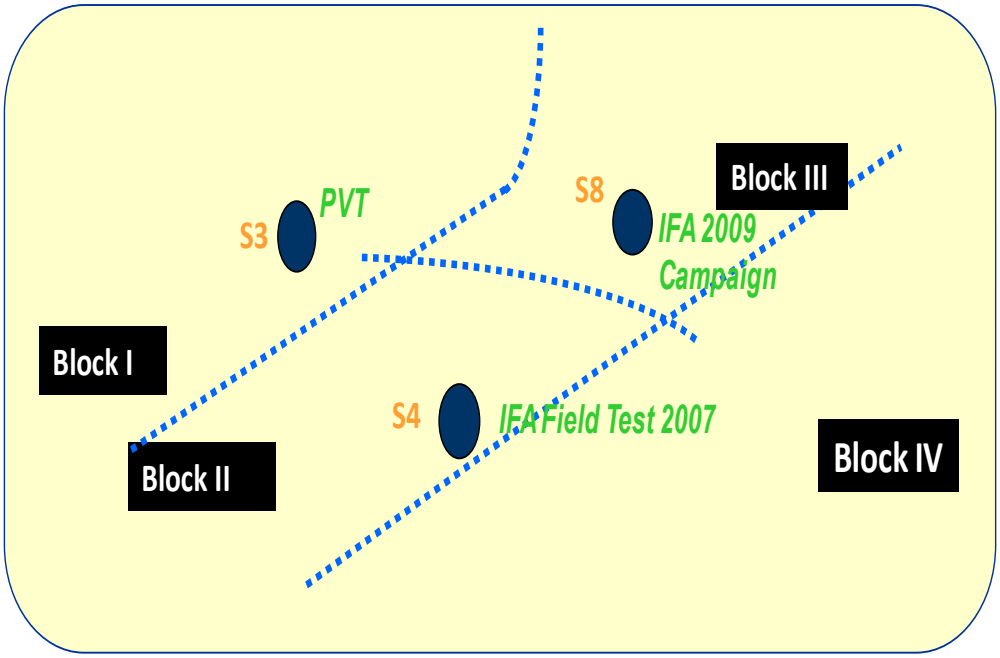

Figure VI.1 – Location of wells with respect to faults. The data collected in wells S3, S4, S8 shall determine connectivity across the faults of block I, II and III.

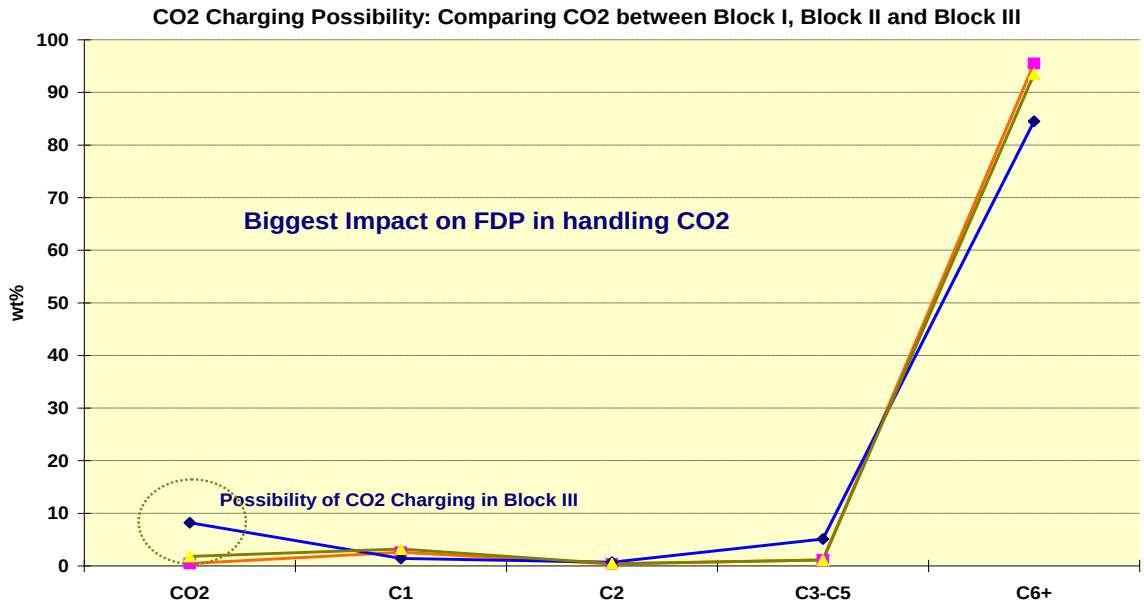

Figure VI.2 – Compositional data based on data and samples collected in wells S3, S4 and S8. (Multalib et al. 2010).

As mentioned earlier, the oil found in this reservoir is low in GOR. That means that the heavier ends dominate the composition with regards to the light ends. Figure VI.2 plots the weight fractions of the light ends on a scale of 0% to 100%. Considering the choice of scale and the fact that these are compositions of black oils, it is not surprising to find that the composition of all light ends overlay. The difference in CO2 content in one well is marked as an outlier. A comment contemplates the possibility of CO2 charging into the reservoir. Even though the large gradient in CO2 is noticed as shown in Figure V.9, no further investigation of the CO2 gradient is presented in the literature.

As pointed out in Chapter III, black oil can have the tendency to be less graded to the point that it appears uniform throughout the column. The composition of black oil can thus be of lesser use to determine connectivity across a fault barrier. The modeling of the case in Chapter IV has shown how useful it can be to consider the CO2 gradient. The CO2 is out of equilibrium and thus appears hard to model or understand. The non-equilibrium simulations of this work can help to understand this gradient. CO2 is the component that exhibits the biggest gradient. The first of the recommendations of this work is to always consider the component that exhibits the largest gradient, even if it can not be modeled with an EoS. The reason for fluid complexities lies in the history of the reservoir. Reservoir mixing processes will try to reduce gradients with time. The component that has the biggest gradient is likely to give evidence of processes that reach further back in time.

The efforts in Chapter V to match the data points have shown that sealing faults can manifest themselves in step changes in composition. These step changes are distinct compared to the smooth curve in case of non sealing faults. It is evident that a small amount of data points can hide this distinct characteristic in the gradients. Hence the second recommendation is: If possible, collect at least two data points per pool/fault-block. A greater number of data points helps to reveal the shape of the gradients, especially in the presents of faults. By nature non-equilibrium gradients are hard to predict as they generally do not follow analytical equations. The deviation from the analytical prediction is what reveals the presence of non-equilibrium. This condition should automatically raise the desire to collect enough data to be able to extract the

information necessary and to make a confident interpretation. Additional measurements will help to better determine the shape of non-equilibrium gradients and eliminate the possibility to misinterpret the data in the presence of faults.

Conclusions

1) A method of modeling non equilibrium gradients has been presented. The simplicity of the model allows the simulation of reservoir fluid mixing processes over time periods of geologic scale.
2) The simplicity inheritably limits the model to only allow assumptions of zeroth order.
3) Efforts to refine the model are focused on realistic assumptions on the diffusion process. Diffusive mixing in a reservoir still bears many uncertainties. Some of the interaction between the rock and the fluid in the context of diffusion will remain hard to quantify. Linear scaling of the diffusion coefficients allows to account for these effects if some quantification becomes available.
4) The model is robust against changes in geometry. The influence of changes in porosity and permeability has been studied. The results reveal an idiosyncrasy of the modeling software. It is important to fully understand the math behind the calculations of diffusivity and transmissivity. The behavior of these calculations with respect to porosity and permeability has no implications on real cases as porosity and permeability are linked statistically.

5) Details of actual present day fluid composition, actual length scales, actual rock properties, reservoir conditions of temperature and pressure, and other detailed information will help to better the approximation of the model. Such further refinement of the model can give more confidence on the actual time frame of the processes. These properties can be seen as dials that may be turned to scale the time to reach equilibrium. The actual shape of the gradients will remain similar in all cases, as they depend on baffles and flow barriers like faults. In most cases, the age and timeframe of the processes and elements of the petroleum system are only known to an approximation.
6) The model tries to give order-of-magnitude-answers to questions about the origin of fluid complexities. The resulting shapes of the gradients help to understand non-equilibrium conditions where the analytical prediction of fluid gradients fails.
7) Guidelines on DFA data acquisition are given, with the intent to better qualify the shape of non-equilibrium fluid gradients.
8) Future work in this area will include the study of not only vertical gradients, but also lateral evolution of gradients in two dimensional models.
9) Pressure communication is necessary, but insufficient to prove compartment connectivity. Quantification of the difference in time for pressure equilibration and compositional equilibration to take place is found to be several orders of magnitude. Further studies are necessary to give hard numbers on the difference between the two.

The more we study fluid columns, the more we understand their complexities. Where analytical equations reach the limit, non-equilibrium modeling leads the way to new insights.

REFERENCES

Al-Meshari, A.A., Aquilar-Zarita, R.A., and McCain, W.D. 2005. Tuning an Equation of State–The Critical Importance of Correctly Grouping Composition into Pseudocomponents. Paper SPE 96416 presented at the SPE Annual Technical Conference and Exhibition, Dallas, Texas, 9 October DOI: 10.2118/96416-MS

Al-Meshari, A.A., and McCain, W.D. 2005. New Strategic Method to Tune Equation-of-State for Compositional Simulation. Paper SPE-106332 presented at the SPE Technical Symposium of Saudi Arabia Section, Dhahran, Saudi Arabia, 14-16 May DOI: 10.2118/106332-MS.

Al-Meshari, A.A., and McCain, W.D. 2006. An Accurate Set of Correlations for Calculating Critical Properties and Acentric Factors for Single Carbon Number Groups. Paper SPE 106338 presented at the SPE Technical Symposium of Saudi Arabia Section, Dhahran, Saudi Arabia 21-23 May DOI: 10.2118/106338-MS.

Al-Meshari, A.A., and McCain, W.D. 2007. Validation of Splitting the Hydrocarbon Plus Fraction First Step in Tuning Equation-of-State. Paper SPE 104631 presented at the SPE Middle East Oil and Gas Show and Conference, Kingdom of Bahrain, 11-14 March DOI: 10.2118/104631-MS.

Betancourt, S.S., Dubost, F.X., Mullins, O.C. et al. 2007. Predicting Downhole Fluid Analysis Logs to Investigate Reservoir Connectivity. Paper SPE 11488 presented at the International Petroleum Technology Conference, Dubai, U.A.E 4-6 December DOI: 10.2523/11488-MS.

Betancourt, S.S., Fujisawa, G., Mullins, O.C. et al. 2004. Exploration Applications of Downhole Measurement of Crude Oil Composition and Fluorescence. Paper SPE 87011 presented at the SPE Asia Pacific Conference on Integrated Modelling for Asset Management, Kuala Lumpur, Malaysia 29-30 March DOI: 10.2118/87011-MS.

Boving, T.B., and Grathwohl, P. 2001. Tracer Diffusion Coefficients in Sedimentary Rocks: Correlation to Porosity and Hydraulic Conductivity. *Journal of Contaminant Hydrology* **53** (1-2): 85-100 DOI: 10.1016/S0169-7722(01)00138-3.

Canas, J.A., Pop, J.J., Dubost, F.X. et al. 2008. Advanced Pressure and Fluid Gradient Analysis of a Deep Offshore Reservoir. Paper SPE 115429 presented at the SPE Annual Technical Conference and Exhibition, Denver, Colorado, 21-24 September DOI: 10.2118/115429-MS.

Cavett, R.H., 1962. Physical Data for Distillation Calculations: Vapor-Liquid Equilibrium. *Proc.* 27th annual meeting American Petroleum Institute, Dallas, Texas, 351-366.

Contreiras, K.D., Van-Duinem, F., Weinheber, P. et al. 2008. Improved Techniques for Acquiring Pressure and Fluid Data in a Challenging Offshore Carbonate Environment. Paper SPE 115504 presented at the SPE Annual Technical Conference and Exhibition, Denver, Colorado, 21–24 September DOI: 10.2523/115504-MS.

Curtiss, C.F., and Bird, R.B. 1999. Multicomponent Diffusion. *Industrial & Engineering Chemistry Research* **38** (7): 2515-2522.

Darken, L.S., 1948. Diffusion, Mobility and Their Interrelation through Free Energy in Binary Metallic Systems. *Transactions of The American Institute of Mining And Metallurgical Engineers* **175**: 184-201.

Dong, C., O'Keefe, M.D., Elshahawi, H. et al. 2008. New Downhole-Fluid-Analysis Tool for Improved Reservoir Characterization. *SPE Reservoir Evaluation & Engineering* **11** (6): 1107-1116.

Dubost, F.X., Carnegie, A.J.G., Mullins, O.C. et al. 2007. Integration of in-Situ Fluid Measurements for Pressure Gradients Calculations. Paper SPE 108494 presented at the International Oil Conference and Exhibition, Veracruz, Mexico 27-30 June DOI: 10.2118/108494-MS.

Dykhuizen, R.C., and Casey, W.H. 1989. An Analysis of Solute Diffusion in Rocks. *Geochimica et Cosmochimica Acta* **53** (11): 2797-2805.

Elshahawi, H., Hashem, M.N., Mullins, O.C. et al. 2005. The Missing Link-Identification of Reservoir Compartmentalization through Downhole Fluid Analysis. Paper SPE 94709 presented at the SPE Annual Technical Conference and Exhibition, Dallas, Texas 9-12 October DOI: 10.2118/94709-MS.

Elshahawi, H., Hows, M.P., Dong, C. et al. 2007. Integration of Geochemical, Mud Gas and Downhole Fluid Analyses for the Assessment of Compositional Grading - Case Studies. Paper SPE 109684 presented at the SPE Annual Technical Conference and Exhibition, Anaheim, California, 11-14 November DOI: 10.2118/109684-MS.

England, W.A., Mackenzie, A.S., Mann, D.M. et al. 1987. The Movement and Entrapment of Petroleum Fluids in the Subsurface. *Journal of the Geological Society* **144** (2): 327-347.

England, W.A., Muggeridge, A.H., Clifford, P.J. et al. 1995. Modelling Density-Driven Mixing Rates in Petroleum Reservoirs on Geological Time-Scales, with Application to the Detection of Barriers in the Forties Field (Ukcs). *Geological Society, London, Special Publications* **86** (1): 185-201.

Fitzgerald, P. 2008. Wireline "Creep". Paper SPE 118027 presented at the Abu Dhabi International Petroleum Exhibition and Conference, Abu Dhabi, U.A.E. 3-6 November DOI: 10.2118/118027-MS

Fitzgerald, P., and Pedersen, B.K. 2007. A Technique for Improving the Accuracy of Wireline Depth Measurements. Paper SPE 110318 presented at the SPE Annual Technical Conference and Exhibition, Anaheim, California, 11-14 November DOI: 10.2118/110318-MS

Freed, D.E., 2007. Dependence on Chain Length of NMR Relaxation Times in Mixtures of Alkanes. *The Journal of Chemical Physics* **126** (17): 174502.

Freed, D.E., 2009. Temperature and Pressure Dependence of the Diffusion Coefficients and NMR Relaxation Times of Mixtures of Alkanes. *The Journal of Physical Chemistry B* **113** (13): 4293-4302.

Freed, D.E., Burcaw, L., and Song, Y.-Q. 2005. Scaling Laws for Diffusion Coefficients in Mixtures of Alkanes. *Physical Review Letters* **94** (6): 067602-1-4.

Freed, D.E., Mullins, O.C., and Zuo, J.Y. 2010. Theoretical Treatment of Asphaltene Gradients in the Presence of GOR Gradients. *Energy & Fuels* **24** (7): 3942-3949.

Fujisawa, G., Mullins, O.C., Dong, C. et al. 2003. Analyzing Reservoir Fluid Composition in-Situ in Real Time: Case Study in a Carbonate Reservoir. Paper SPE 84092 presented at the SPE Annual Technical Conference and Exhibition, Denver, Colorado, 5-8 October DOI: 10.2118/84092-MS.

Grathwohl, P., 1998. *Diffusion in Natural Porous Media: Contaminant Transport, Sorption/Desorption and Dissolution Kinetics.* Topics in Environmental Fluid Mechanics. Boston: Kluwer Academic Publishers.

Grogan, A.T., Pinczewski, V.W., Ruskauff, G.J. et al. 1988. Diffusion of CO2 at Reservoir Conditions: Models and Measurements. *SPE Reservoir Engineering* **3** (1): 93-102.

Harfoushian, J.H., Daungkaew, S., Cheong, B.C. et al. 2008. First Field Application of Downhole CO2 Measurement in Asia Pacific. Paper SPE 116501 presented at the SPE Asia Pacific Oil and Gas Conference and Exhibition, Perth, Australia, 20-22 October DOI: 10.2118/116501-MS.

Hashem, M., Elshahawi, H., and Ugueto, G. 2004. A Decade of Formation Testing - Do's and Don'ts and Tricks of the Trade. Paper presented at the SPWLA 45th Annual Logging Symposium, Noordwijk, The Netherlands, June 6-9.

Hoier, L., and Whitson, C.H. 2001. Compositional Grading - Theory and Practice. *SPE Reservoir Evaluation & Engineering* **4** (6): 525-535.

Jamialahmadi, M., Emadi, M., and Müller-Steinhagen, H. 2006. Diffusion Coefficients of Methane in Liquid Hydrocarbons at High Pressure and Temperature. *Journal of Petroleum Science and Engineering* **53** (1-2): 47-60.

Jackson, R.R., Carnegie, A., and Dubost, F.X. 2007. Pressure Measurement and Pressure Gradient Analysis: How Reliable for Determining Fluid Density and Compositional Gradients? Paper SPE 111911 presented at the Nigeria Annual International Conference and Exhibition, Abuja, Nigeria, 6-8 August DOI: 10.2118/111911-MS.

Kabir, C.S., and Pop, J.J. 2007. How Reliable Is Fluid Gradient in Gas/Condensate Reservoirs? *SPE Reservoir Evaluation & Engineering* **10** (6): 644-656.

Liu, H., and Macedo, E.A. 1995. Accurate Correlations for the Self-Diffusion Coefficients of CO2, CH4, C2H4, H2O, and D2O over Wide Ranges of Temperature and Pressure. *The Journal of Supercritical Fluids* **8** (4): 310-317.

Montel, F., Bickert, J., Hy-Billiot, J. et al. 2003. Pressure and Compositional Gradients in Reservoirs. Paper SPE 85668 presented at the Nigeria Annual International Conference and Exhibition, Abuja, Nigeria, 4-6 August DOI: 10.2118/85668-MS.

Muggeridge, A.H., and Smalley, P.C. 2008. A Diagnostic Toolkit to Detect Compartmentalization Using Time-Scales for Reservoir Mixing. Paper SPE 118323 presented at the Abu Dhabi International Petroleum Exhibition and Conference, Abu Dhabi, U.A.E. 3-6 November DOI: 10.2118/118323-MS.

Mullins, O.C., 2010a. The Modified Yen Model. *Energy & Fuels* **24** (4): 2179-2207.

Mullins, O.C., 2010b. Discussed case of field in Ghana that exhibits all equilibrated fluid column. Gas cap and oil zone are separated by 10m thick shale. Personal Communication, College Station, Texas.

Mullins, O.C., 2008. *The Physics of Reservoir Fluids; Discovery through Downhole Fluid Analysis.* Houston, Texas: Schlumberger.

Mullins, O.C., Cribbs, M.E., Beck, G.F. et al. 2001. Downhole Determination of GOR on Single-Phase Fluids by Optical Spectroscopy. Paper presented at the SPWLA 42nd Annual Logging Symposium, Houston, Texas, June 17-20.

Mullins, O.C., Mitra-Kirtley, S., and Zhu, Y. 1992. The Electronic Absorption-Edge of Petroleum *Applied Spectroscopy* **46** (9): 1405-1411.

Mullins, O.C., and Schroer, J. 2000. Real-Time Determination of Filtrate Contamination During Openhole Wireline Sampling by Optical Spectroscopy. Paper SPE 63071 presented at the SPE Annual Technical Conference and Exhibition, Dallas, Texas, 1-4 October DOI: 10.2118/63071-MS.

Mullins, O.C., Zuo, J.Y., Freed, D.E. et al. 2010. Downhole Fluid Analysis Coupled with Novel Asphaltene Science for Reservoir Evaluation. Paper presented at the SPWLA 51th Annual Logging Symposium, Perth, Australia.

Multalib, T.I.T., Hong, T.Y., Lin, T.G. et al. 2010. An Efficient Way to Characterize Complex Reservoir Fluids through Downhole Fluid Properties Measurement. Poster presented at the Petroleum Geology Conference and Exhibition, Kuala Lumpur, Malaysia, 29-30 March.

O'Keefe, M.D., Eriksen, K.O., Williams, S.M. et al. 2006. Zero Percent Contamination of Reservoir Fluid Samples Achieved by Focused Sampling. Paper SPE 101084 presented at the SPE Asia Pacific Oil & Gas Conference and Exhibition, Adelaide, Australia, 11-13 September DOI: 10.2118/101084-MS.

O'Keefe, M.D., Godefroy, S., Vasques, R.R. et al. 2007. In-Situ Density and Viscosity of Reservoir Fluids Measured by Wireline Formation Testers. Paper SPE 110364 presented at the Asia Pacific Oil and Gas Conference and Exhibition, Jakarta, Indonesia, 30 October-1 November DOI: 10.2118/110364-MS.

Péneloux, A., Rauzy, E., and Fréze, R. 1982. A Consistent Correction for Redlich-Kwong-Soave Volumes. *Fluid Phase Equilibria* **8** (1): 7-23.

Poling, B.E. Prausnitz, J.M. and O'Connell, J.P. 2001. *Properties of Gases and Liquids*. 5th edition. New York: McGraw-Hill.

Riazi, M.R., 1996. A New Method for Experimental Measurement of Diffusion Coefficients in Reservoir Fluids. *Journal of Petroleum Science and Engineering* **14** (3-4): 235-250.

Riazi, M.R., and Al-Sahhaf, T.A. 1996. Physical Properties of Heavy Petroleum Fractions and Crude Oils. *Fluid Phase Equilibria* **117** (1-2): 217-224.

Riazi, M.R., and Whitson, C.H. 1993. Estimating Diffusion Coefficients of Dense Fluids. *Industrial & Engineering Chemistry Research* **32** (12): 3081-3088.

Smits, A.R., Fincher, D.V., Nishida, K. et al. 1995. In-Situ Optical Fluid Analysis as an Aid to Wireline Formation Sampling. *SPE Formation Evaluation* **10** (2): 91-98. 26496-PA.

Stainforth, J.G., 2004. New Insights into Reservoir Filling and Mixing Processes. In *Understanding Petroleum Reservoirs: Towards an Integrated Reservoir Engineering and Geochemical Approach*, ed. J.M. Cubitt, W.A. England and S.R. Larter. SP **235**: 115-132. London: Geological Society.

Taylor, R., and Krishna, R. 1993. Multicomponent Mass Transfer Wiley Series in Chemical Engineering. New York: Wiley.

Venkataramanan, L., Gustavson, G., and Weinheber, P. et al. 2006. Pressure Gradients and Fluid Analysis as an Aid to Determining Reservoir Compartmentalization. Paper presented at the SPWLA 47th Annual Logging Symposium, Veracruz, Mexico, June 4-7.

Weinheber, P., and Vasques, R. 2006. New Formation Tester Probe Design for Low Contamination Sampling. Paper presented at the SPWLA 47th Annual Logging Symposium, Veracruz, Mexico, June 4-7.

Weinheber, P., Jackson, R.R., Santo, I.D. et al. 2009. Focused Sampling and Downhole Fluid Analysis with Wireline Formation Testers: Perspective from Offshore West Africa. Paper presented at the Offshore Technology Conference, Houston, Texas, 4-7 May DOI: 10.4043/20024-MS.

Xian, C., Zuo, J.Y., Haddad, S.S. et al. 2010. Reservoir Architecture Characterization: EOS Based Downhole Fluid Analysis, Openhole Logs and Pressures Integration. Paper SPE 130900 presented at the International Oil and Gas Conference and Exhibition in Beijing, China, 8-10 June DOI: 10.2118/130900-MS.

Yuan-Hui, L., and Gregory, S. 1974. Diffusion of Ions in Sea Water and in Deep-Sea Sediments. *Geochimica et Cosmochimica Acta* **38** (5): 703-714.

Zuo, J.Y., Freed, D., Mullins, O.C. et al. 2010. Interpretation of DFA Color Gradients in Oil Columns Using the Flory-Huggins Solubility Model. Paper SPE 130305 presented at the International Oil and Gas Conference and Exhibition in Beijing, China 8-10 June DOI: 10.2118/133656-MS.

Zuo, J.Y., Mullins, O.C., Dong, C. et al. 2009a. Investigation of Formation Connectivity Using Asphaltene Gradient Log Predictions Coupled with Downhole Fluid Analysis. Paper SPE 124264 presented at the SPE Annual Technical Conference and Exhibition, New Orleans, Louisiana, 4-7 October DOI: 10.2118/124264-MS.

Zuo, J.Y., Xian, C., Haddad, S. et al. 2009b. Methodology for Reservoir Complexity Determination from Downhole Fluid Analysis and EOS Predictions. Paper SPE 13163 presented at the International Petroleum Technology Conference, Doha, Qatar, 7-9 December DOI: 10.2523/13163-MS.

Zuo, J.Y., Zhang, D., Dubost, F.X. et al. 2008. EOS Based Downhole Fluid Characterization. Paper SPE 114702 presented at the SPE Asia Pacific Oil and Gas Conference and Exhibition, Perth, Australia, 20-22 October DOI: 10.2118/114702-MS.

VITA

Thomas Pfeiffer received his B.S. in electrical engineering in 1996 and his M.S. in electrical engineering in 2001 from the Technical University of Munich, Germany. He joined Schlumberger as a wireline field engineer in January 2002. Assigned locations include the North Sea, central and eastern Europe and the Gulf of Mexico. As Field Service Manager he was in charge of Schlumberger's wireline operation in Austria, Hungary, Czech Republic, Slovenia and Slovakia from January 2005 to August 2006. Prior to enrolling at Texas A&M he worked as a wireline formation testing engineer in Belle Chasse, Louisiana for three years. During this assignment he deepened his extensive field experience in deepwater wireline formation testing and DFA. In August 2009 Schlumberger sponsored his education at Texas A&M with the goal to receive a Master of Science in petroleum engineering.

Thomas Pfeiffer may be reached at his permanent address: Wallgraben 1, 49696 Molbergen, Germany or via e-mail: tpfeiffer@slb.com.